# Fragment-to-Hit-to-Lead Discovery of a Novel Pyridylurea Scaffold of ATP Competitive Dual Targeting Type II Topoisomerase Inhibiting Antibacterial Agents

Gregory S. Basarab,*[†] John I. Manchester,[†] Shanta Bist,[†] P. Ann Boriack-Sjodin,[†,§] Brian Dangel,[†] Ruth Illingworth,[†] Brian A. Sherer,[†,‖] Shubha Sriram,[†] Maria Uria-Nickelsen,[†,‡] and Ann E. Eakin[†,⊥]

[†]Infection Innovative Medicines, AstraZeneca R&D Boston, 35 Gatehouse Drive, Waltham, Massachusetts 02451, United States
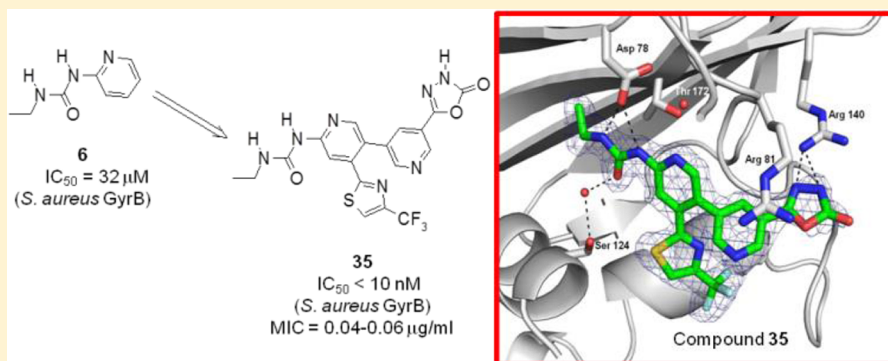
ABSTRACT: The discovery and optimization of a new class of bacterial topoisomerase (DNA gyrase and topoisomerase IV) inhibitors binding in the ATP domain are described. A fragment molecule, 1-ethyl-3-(2-pyridyl)urea, provided sufficiently potent enzyme inhibition (32 μM) to prompt further analogue work. Acids and acid isosteres were incorporated at the 5-pyridyl position of this fragment, bridging to a key asparagine residue, improving enzyme inhibition, and leading to measurable antibacterial activity. A CF$_3$-thiazole substituent at the 4-pyridyl position improved inhibitory potency due to a favorable lipophilic interaction. Promising antibacterial activity was seen versus the Gram-positive pathogens *Staphylococcus aureus* and *Streptococcus pneumoniae* and the Gram-negative pathogens *Haemophilus influenzae* and *Moraxella catarrhalis*. Precursor metabolite incorporation and mutant analysis studies support the mode-of-action, blockage of DNA synthesis by dual target topoisomerase inhibition. Compound **35** was efficacious in a mouse *S. aureus* disease model, where a 4.5-log reduction in colony forming units versus control was demonstrated.

■ INTRODUCTION

The need for novel antibacterials has intensified due to the continuing emergence of resistant bacteria limiting the utility of many drug therapies.[1−5] Since the start of the new millennium, only seven new chemical entities have received FDA approval as systemic antibacterials and, of these, only two, linezolid and daptomycin, operate by novel modes-of-action unrelated to previous drugs.[6] Many new antibiotics brought to the marketplace are active against resistant clinical strains either due to increased potency (as for tigecycline in the tetracycline class of antibiotics)[7] or to decreased susceptibility to the degradation mechanisms (as for the carbapenems).[8,9] However, increased resistance can be expected to develop in due time.

The fluoroquinolone and aminocoumarin classes of antibacterials demonstrate clinical utility via inhibition of the topoisomerases DNA gyrase and topoisomerase IV necessary for DNA replication.[10−12] DNA gyrase and topoisomerase IV are tetrameric A$_2$B$_2$ complexes wherein the A subunits (designated GyrA for DNA gyrase, ParC for topoisomerase IV) contain the DNA cleavage domain while the B subunits (designated GyrB for DNA gyrase and ParE for topoisomerase

IV) contain the ATP binding and hydrolysis domain. Inhibitors of DNA gyrase typically also inhibit bacterial topoisomerase IV, although the relative importance for expression of antibacterial activity can vary depending on the inhibitor and the bacterial species.[13−15] The two most widely sold fluoroquinolones, ciprofloxacin and levofloxacin, have encountered growing resistance mediated by mutations in one or both of the targets since their FDA approvals in 1987 and 1996, respectively.[16,17] While fluoroquinolones bind to the DNA cleaved complex of DNA gyrase and topoisomerase IV, the natural product aminocoumarins, clorobiocin and novobiocin, instead inhibit ATPase activity in the GyrB and ParE subunits.[18,19] Aminocoumarins have not received widespread usage due to poor pharmacokinetic properties and issues of safety, and therefore widespread clinical resistance has not materialized.[12,18]

In addition to aminocoumarin antibiotics, a wide variety of compound scaffolds exist from synthetic and biological sources that bind in the ATP binding pocket of GyrB/ParE and result
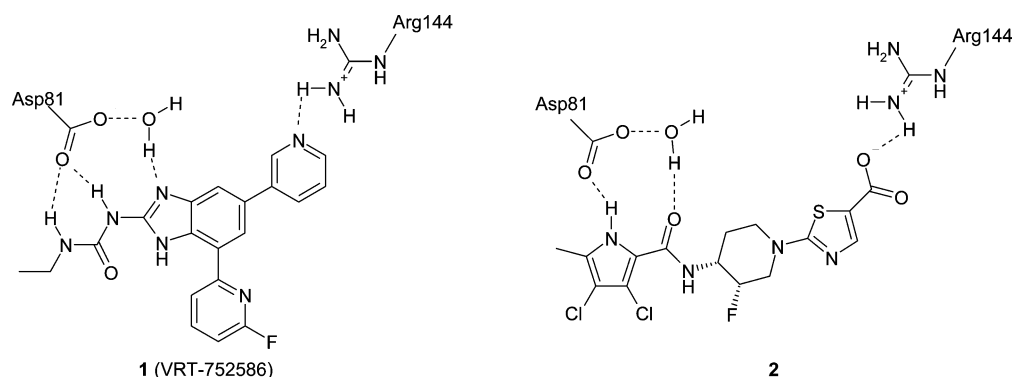
Figure 1. Hydrogen bonding array around urea and pyrrolamide inhibitors.

in antibacterial activity.[20] This would include cyclothialidine,[21] a natural product distinct from the aminocoumarins, a related synthetic scaffold that afforded in vivo efficacy[22] and a rhodanine derivative that maintained a part of the cyclothialidine pharmacophore.[23] Efforts to mimic the adenine of ATP have led to an aminopyrazolopyrimidine replacement.[24] Recent substituted pyrrolopyrimidines,[25] azaindoles,[26] and bithiazoles[27] invoke scaffold hopping approaches to derive novel structural motifs. An anilinopyrimidine class of GyrB/ParE inhibitor was derived by finding a hit through screening a corporate compound collection in a ParE ATPase assay.[28] There are at least four types of fused bicyclic scaffolds incorporating a urea pharmacophore,[29−33] including the benzimidazole urea class of antibacterials as in VRT-752586 (**1**, Figure 1).[29] The use of fragments or low-molecular-weight compounds to identify starting points for the design DNA gyrase inhibiting antibacterials has proven useful[33−35] and has led to the pyrrolamide class of antibacterials such as **2** (Figure 1).[36]

X-ray crystallographic structures have shown that **1** and **2** each occupy the position of the adenine portion of ATP with hydrogen bonds donating and receiving interactions with Asp81 (*Staphylococcus aureus* DNA gyrase numbering) and a conserved water molecule.[29,35] Compared to the ATP binding interactions determined from an *Escherichia coli* X-ray cocrystal structure of a 43 kDa GyrB domain and a nonhydrolyzable ATP analogue,[37] both **1** and **2** extend outside of the ATP pocket to form hydrogen bonds or a salt bridge to the side chain of Arg144 (see Figure 1). With this information in hand, another scaffold was desired that would bind similarly to the adenine binding domain and form a hydrogen bond or salt bridge to the guanidine moiety of Arg144. A novel scaffold allows for the display of diverse functionality in the ATP binding pocket, thereby differentiating the structure−activity parameters that can be explored relative to other antibacterials targeting topoisomerase ATPase domains.

A hybrid design was envisioned where a urea interaction with Asp81 as with **1** and a salt bridge to Arg144 as with **2** would be linked in the same molecule. To this end, previously unexplored 2-pyridylureas were chosen for investigation wherein the heterocycle nitrogen is positioned for a hydrogen bond to the crystallographic water molecule similar to the benzimidazole nitrogen of **1**. Molecular modeling was carried out after removing the ligand from a *S. aureus* DNA GyrB structure (3U2K, the N-terminal domain including a loop deletion residues 14−104 and 128−233)[35] and docking a 2-pyridylurea. The pose shows that substitution at the pyridyl 5-position (see Figure 2 for numbering) reaches toward Arg144
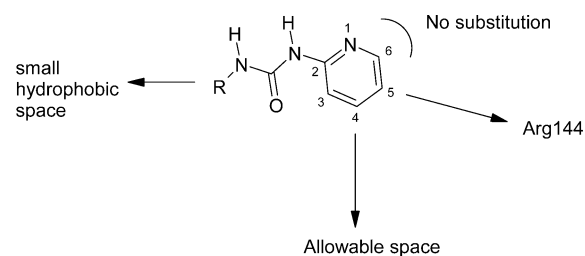

Figure 2. Design features of pyridylureas.

with a properly positioned carboxylate, and substitution at the pyridyl 4-position allows exploration into a more open region that extends toward the binding site for the ATP ribose ring. The pyridyl 6-position abuts a hydrophobic surface of the enzyme and should not be substituted nor replaced with a heteroatom. The urea substituent approaches a small hydrophobic space that allows for small complementary hydrophobic substituents as with compound **1**. Other monocyclic heterocycles, in particular those with 5-membered rings such as imidazoles and furans, were discounted as it was difficult to build a straightforward trajectory that would allow an interaction with Arg144 and avoid steric clashes with the enzyme. Here, we describe the progression of a set of fragment compounds with modest biochemical inhibition and favorable ligand efficiencies to a viable lead, which we denote as demonstrating promising antibacterial activity and efficacy in an animal disease model.

■ CHEMISTRY

A set of monocyclic aryl urea fragments (Figure 3) was tested for ATPase inhibitory activity of a hybrid DNA gyrase containing two *S. aureus* GyrB units and two *E. coli* GyrA units.[35] The compounds were commercially available or synthesized by reacting alkyl isocyanates with aminoheterocycles or alkylamines with the phenylcarbamate of aminopyridine. This survey led to ethyl-pyridylurea **6** being chosen as the starting point for elaboration. Compounds were synthesized (see Tables 1−3) to investigate the influence of 5-position substitutions designed to extend toward Arg144 and 4-position substitutions to fill the allowable space abutting the ATP ribose binding region. Scheme 1 shows the synthesis of **14**, carried out straightforwardly in four steps by formation of ether **43** followed by reaction with ethylisocyanate forming the urea and ester hydrolysis.

For the synthesis of compounds **15−23**, an aryl group was attached directly to the pyridylurea core at the 5-position as
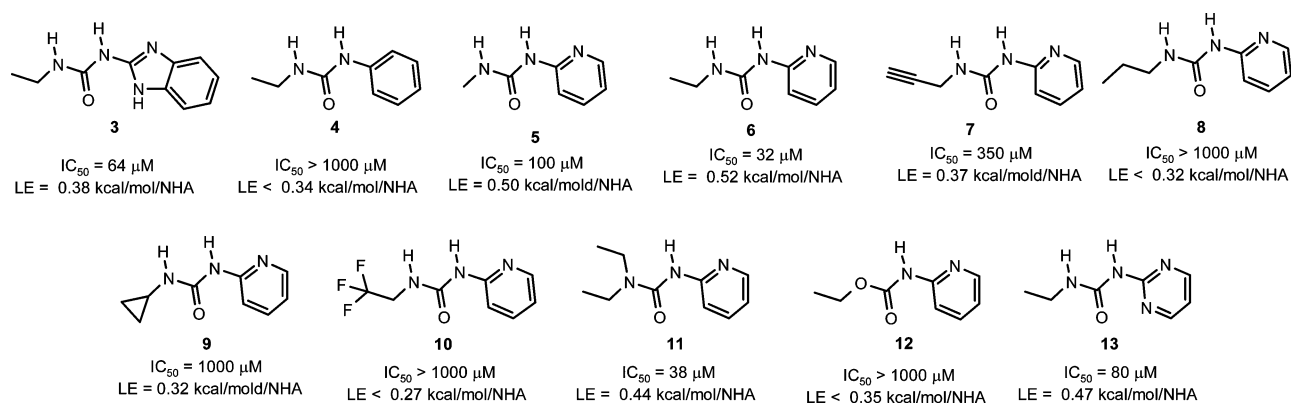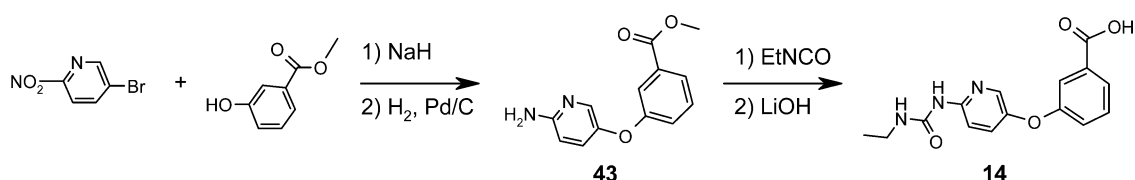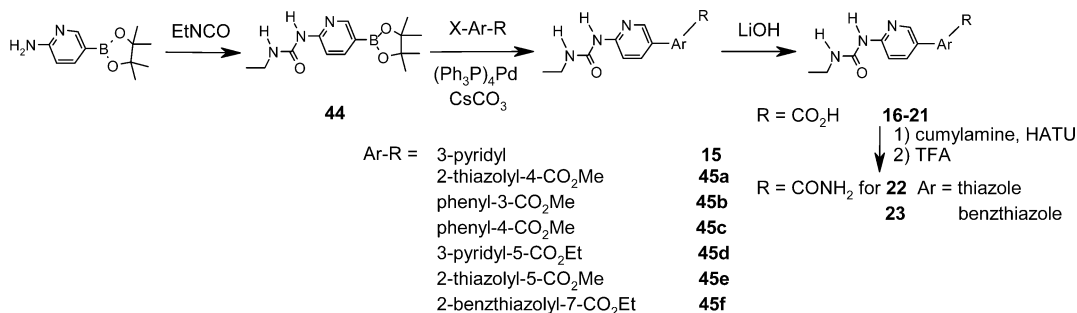
Figure 3. IC$_{50}$s and ligand efficiencies (LE) of urea fragments versus *S. aureus* ATPase activity.

Scheme 1. Synthesis of Compound 14

Scheme 2. Synthesis of Compounds 15−23

Ar-R =	3-pyridyl	15
	2-thiazolyl-4-CO$_2$Me	45a
	phenyl-3-CO$_2$Me	45b
	phenyl-4-CO$_2$Me	45c
	3-pyridyl-5-CO$_2$Et	45d
	2-thiazolyl-5-CO$_2$Me	45e
	2-benzthiazolyl-7-CO$_2$Et	45f

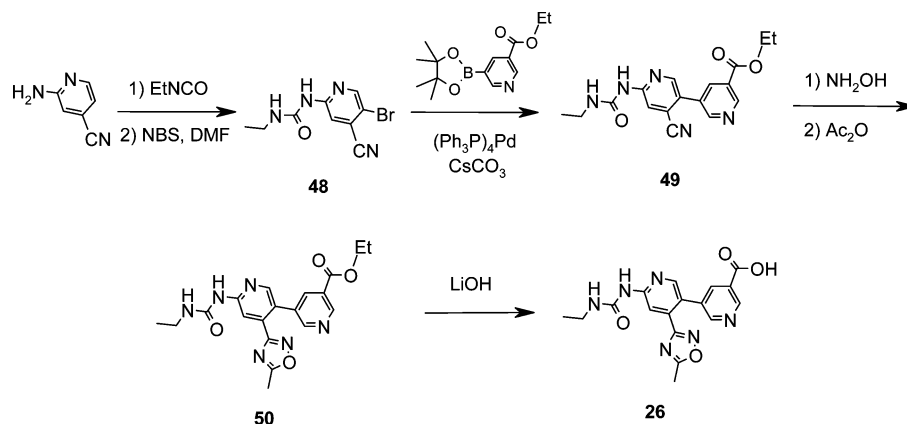**Scheme 3. Synthesis of Compounds 24−25**
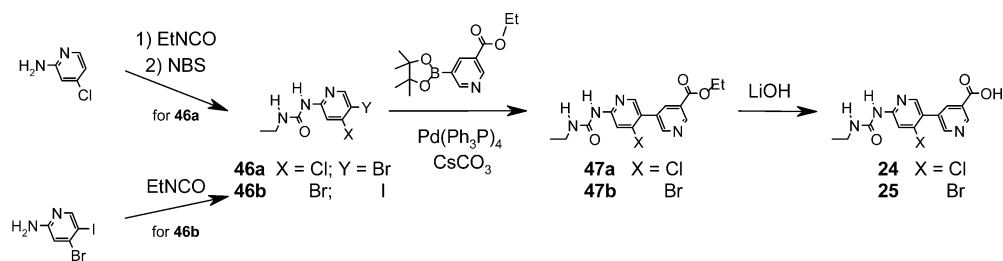
outlined in Scheme 2. Addition of ethylisocyanate to the pinacol ester of 2-aminopyridine-5-boronic acid afforded **44**; subsequent treatment with arylhalides in palladium catalyzed cross-coupling reactions afforded **15** and esters **45a−f**. Hydrolysis of esters afforded the corresponding acids **16−21** targeted to form the salt bridge to Arg144. In two instances, the acids were converted to amides (compounds **22** and **23**) by conversion to the cumylamide and TFA removal of the cumyl group. Overall, Suzuki cross-couplings constituted the primary method for the assembly of such biaryl units that ultimately link the urea pharmacophore with an acid or acid isoster pharmacophore. The electrophilic component of the cross-coupling lies on the pyridyl urea core, while the nucleophilic

component is on the appended aryl ring that extends toward Arg144.

A series of analogues was assembled with substituents at the pyridyl 5-position and phenyl or pyridyl acids at the 4-position as diagrammed in Schemes 3−6. The electrophilic and nucleophilic components were reversed relative to Scheme 2 with coupling of a bromo or iodo pyridylurea with aryl boronates. Scheme 3 shows the synthesis of compounds **24** and **25** starting by preparation of **46a** and **46b**. The differential halogen substitutions allowed for selective palladium catalyzed cross-coupling of the commercially available pinacol ester of 3-ethoxycarbonylpyridine-5-boronic acid with the requisite dihalopyridyl ureas, leading to **47a** and **47b**. Subsequent hydrolysis afforded **24** and **25**, where the halogen atoms are

Scheme 4. Synthesis of Compound 26

Scheme 5. Synthesis of Compounds 27−29
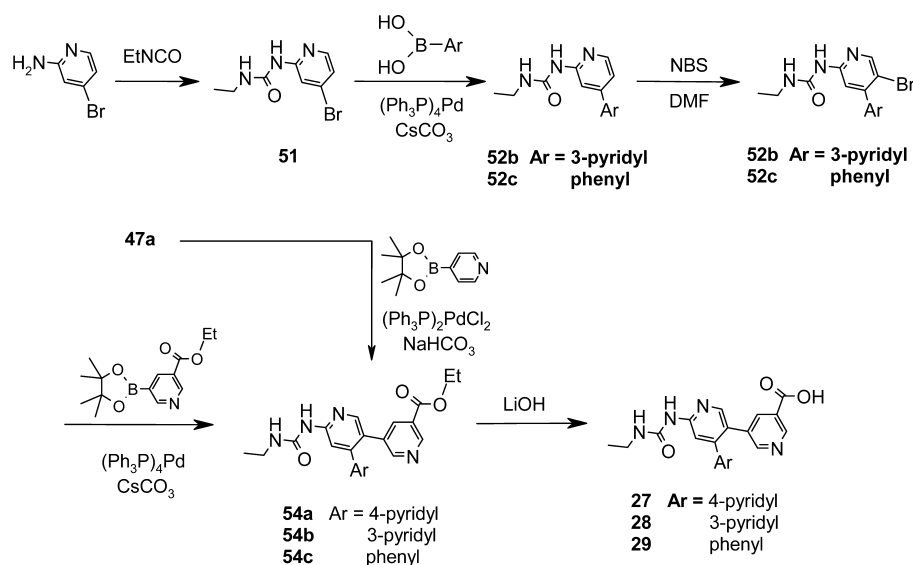
directed toward the allowable space shown in Figure 2. For these and most of the subsequent analogues, the 3,3-bipyridyl scaffold was utilized as it proved to afford overall higher enzyme inhibitory potency and lower MIC values relative to other bipyridyl scaffolds (data not shown).

The chemistries in Schemes 4−6 focus on building onto the pyridyl urea 4-position where, in part, the ribose ring of ATP resides. In Scheme 4, the nitrile serves as a synthetic handle for incorporation of an oxadiazole ring. The aminoisopicolinonitrile was converted in two steps to bromide **48**, setting up a palladium catalyzed cross-coupling reaction with the pyridyl-boronate to afford **49**. The nitrile was converted to the isoxadiazole ring in **50**, and the ester was hydrolyzed to the acid of **26**.
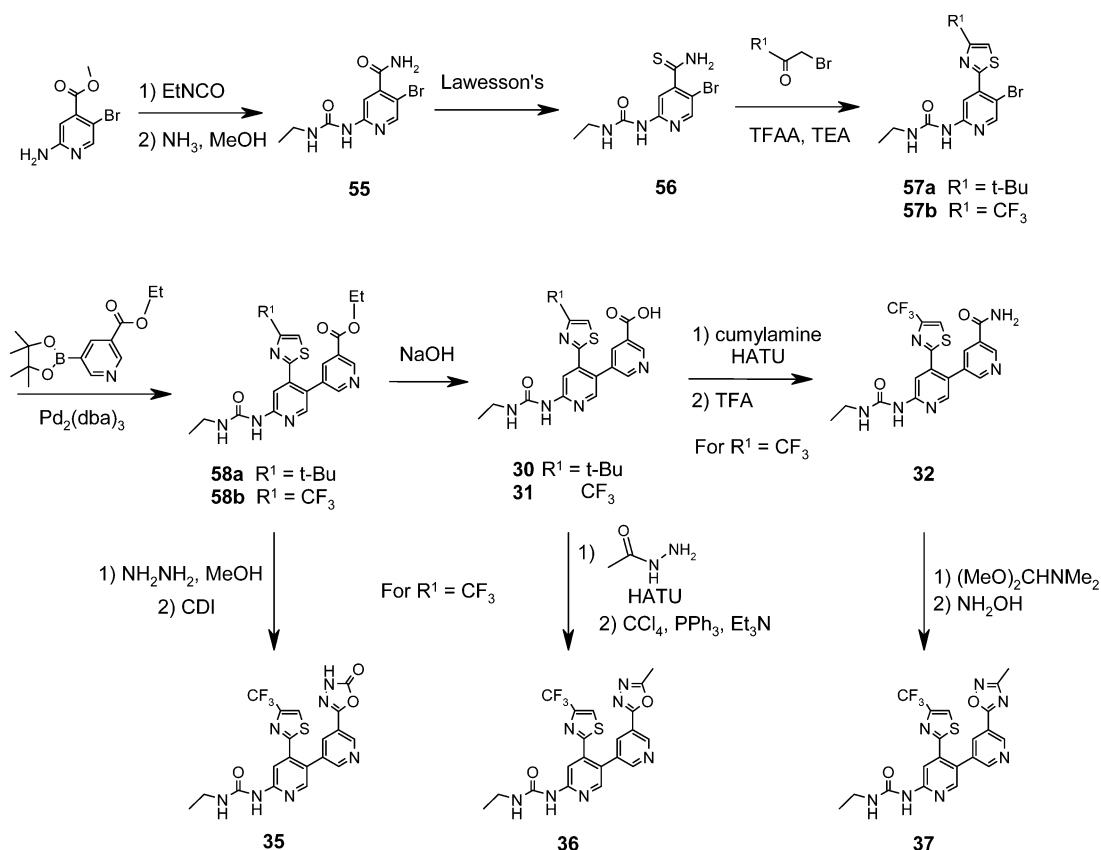
Scheme 5 outlines the synthesis of analogues with a variety of aromatic groups at the pyridyl 4-position and a 3-pyridylcarboxylic acid at the 5-position. Compound **54a** was made from **47a** by Suzuki reaction with the pinacol ester of 4-pyridylboronic acid. For the other two compounds in Scheme 5, 2-amino-4-bromopyridine was first capped with ethylisocyanate, allowing for palladium catalyzed arylation affording compounds **52b** and **52c**. Bromination proceeded selectively at the 5-position of the pyridine setting the stage for a second palladium catalyzed arylation affording compounds **54b** and

54c. The esters of **54a−c** were subsequently hydrolyzed to the acids **27−29**.

Thiazole rings were introduced at the pyridylurea 4-position starting by reaction of methyl 2-amino-5-bromopyridine-4-carboxylic acid with ethylisocyanate and aminolysis of the ester to afford **55** as shown in Scheme 6. After converting the amide of **55** to the thioamide, reaction with bromoketones and dehydration led to compounds **57a** and **57b**. Suzuki arylation and ester hydrolysis afforded compounds **30** and **31**. Analogues with alternative functionality to the acid of **31** were targeted; the ester of **58b** was treated with hydrazine and carbonyl diimidazole to afford oxadiazolone **35**. The acid of **31** was coupled with acetylhydrazide followed by dehydration to afford oxadiazole **36**. The acid of **31** was also converted to amide **32** by coupling with cumylamine followed by TFA solvolysis, and the amide was converted to oxadiazole **37** by formation of the intermediate acylamidine with Brederick's reagent and subsequent treatment with hydroxylamine.

To build compounds with thiazoles at the pyridylurea 4-position and thiazoles/benzthiazoles at the 5-position, Suzuki reactions required the electrophilic boronate partner to reside on the pyridine while the nucleophilic halide resides on the thiazole and benzthiazole (see Scheme 7). To this end, **57b** was converted to the boronate **59**, allowing for cross-coupling with

Scheme 6. Synthesis of Compounds 30−32, 35−37

Scheme 7. Synthesis of Compounds 33−34
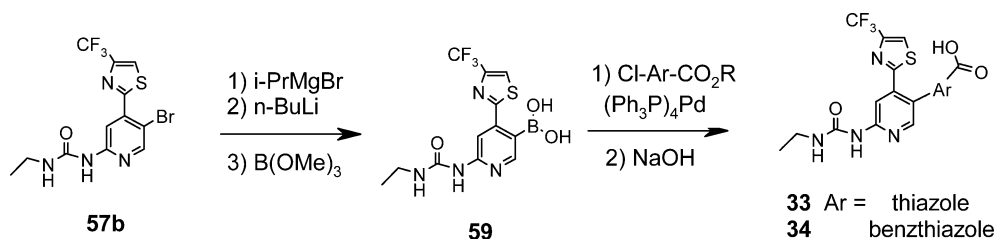
the requisite chlorothiazole and chlorobenzthiazole, setting up the subsequent hydrolysis to afford acids **33** and **34**.

Outlined in Scheme 8 is the synthesis of several additional analogues with functionality alternative to the acid envisioned to reach out to Arg144. Two sequential Suzuki cross-coupling reactions starting from compound **57b** allowed formation of isoxazole **38**. Cross-coupling of the pinacol ester of 5-cyano-3-pyridyl boronic acid with **57b** led to **39**; the nitrile was subsequently converted to the tetrazole of **40**. Compound **39** was also treated with hydroxylamine to form hydroxyamidine **41**; subsequent reaction with carbonyl diimidazole afforded oxadiazolone **42**.

■ RESULTS AND DISCUSSION

The pyrrolamide antibacterial class of DNA gyrase inhibitors (e.g., **2**) was derived from NMR-based screening of a fragment library and led to the identification of a pyrrole carboxylic ester with a K_D = 1.1 mM against an *E. coli* N-terminal 24 kDa ATP-binding domain.[35,36] In a similar approach, inhibitory potency (IC$_{50}$, or the concentration at which ATPase activity was reduced to 50%) for 11 readily available arylurea fragments was

measured (Figure 3). The aim of this fragment approach was to assess the constraints in the adenine binding region before embarking on an extensive analogue campaign. Five of the compounds showed IC$_{50}$ values less than 100 μM and ligand efficiencies (LE) greater than 0.38 kcal/mol/N.[38] Benzimidazole urea **3**, a positive control fragment of **1**, displayed low micromolar potency as expected. Phenylurea **4**, lacking a heterocyclic nitrogen deemed important for the hydrogen bonding array with the conserved crystallographic water molecule, served as a negative control, and accordingly, did not inhibit activity at 1 mM, the highest concentration tested. The ethylurea substituent of **6** produced the highest potency and highest LE of the fragment set in line with the motif reported for the benzimidazole ureas as in **1**. The smaller methylurea **5**, although 2.5-fold less potent, nearly matched the LE of **6**. Substituents larger than ethyl on the urea were disfavored for both potency and, consequently, LE. Notably, a measure of branching with the cyclopropylurea substituent of **9** was not well-tolerated for activity. Compounds **11** and **12** were evaluated to determine the effect of eliminating the distal urea hydrogen bond donors to Asp81, with the diethylurea **11**
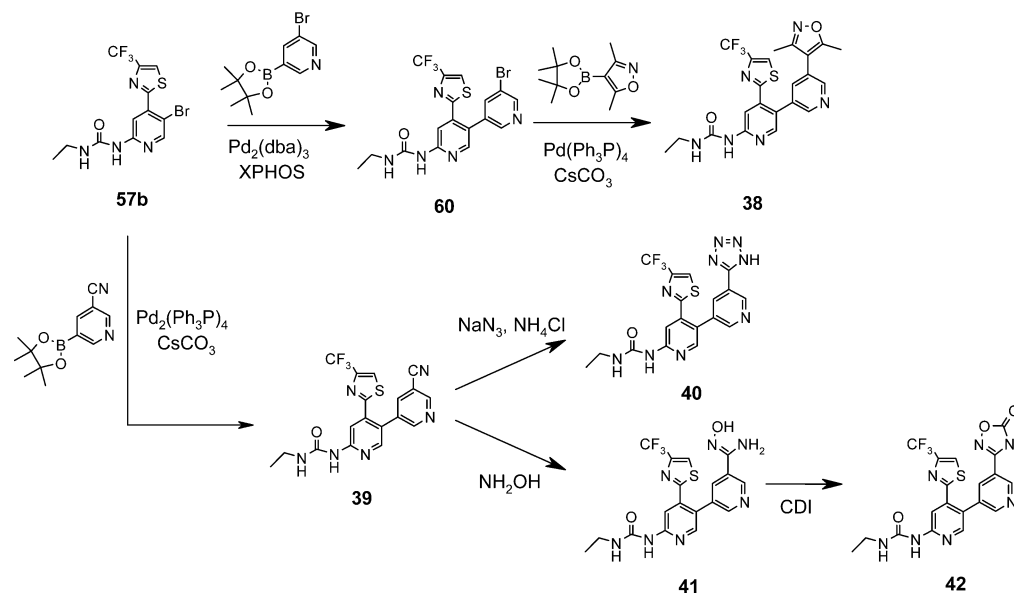
Scheme 8. Synthesis of Compounds 38−40

Table 1. Isozyme Inhibition and MIC Values for 5-Substitited Pyridylureas

Cmpd	R5	Sau[a] GyrB IC$_{50}$ (µM)	Eco GyrB IC$_{50}$ (µM)	Eco ParE IC$_{50}$ (µM)	Spn ParE IC$_{50}$ (µM)	MIC (µg/ml)[b]						
						S. pneumoniae	MSSA[c] *S. aureus*	MRQR[d] *S. aureus*	*M. catarrhalis*	*H. influenzae*	*E. coli*	*E. coli tolC*
14		9.9	4.4	>200	16	>64	>64	>64	>64	>64	>64	>64
15		2.7	2.0	80	1.4	-	>48	>64	>48	>48	>48	>48
16		3.6	-	-	-	>64	>64	>64	>64	>64	>64	-
17		3.4	4.7	69	2.0	21	>64	>64	42	59	>64	>64
18		0.88	1.6	28	0.054	-	>64	>64	4	16	>64	16
19		0.85	1.4	24	0.40	>64	>64	>64	>64	>64	>64	>64
20		0.27	0.24	8.8	0.11	64	>64	>64	>64	>64	>64	-
21		0.10	-	2.1	-	2	>64	>64	8	16	>64	8
22		0.55	0.56	27	0.38	4	64	>64	8	32	>64	16
23		0.039	0.094	12	0.071	1	>64	>64	>64	>64	>64	>64

[a]Sau, Eco, and Spn indicate the enzymes from *S. aureus*, *E. coli*, and *S. pneumoniae*, respectively. [b]Bacterial strains are described in experimental procedures. [c]Methicillin sensitive *S. aureus*. [d]Methicillin resistant, quinolone resistant.

showing that elimination of one H-bond donor can be compensated by increasing hydrophobicity. The lower potency of carbamate 12 showed, however, the H-bond acceptor is not tolerated. The isomeric carbamate of 12 where the side chain oxygen and nitrogen atoms are transposed (the pyridyloxy *N*-

ethylcarbamate) was synthesized, but it was too unstable in solution for evaluation. Finally, the pyrimidine urea 13 showed 2-fold lower potency than 6; presumably the lower lipophilicity imparted by the additional heterocyclic nitrogen does not contribute to a binding interaction with the enzyme. On the

Table 2. Influence of Pyridylurea 4-Position on Isozyme Inhibition and MIC Values

Cmpd	R4	R5	logD	Sau[a] GyrB IC$_{50}$ (μM)	Eco GyrB IC$_{50}$ (μM)	Eco ParE IC$_{50}$ (μM)	Spn ParE IC$_{50}$ (μM)	MIC (μg/ml)[b]						
								S. pneumoniae	MSSA[c] S. aureus	MRQR[d] S. aureus	M. catarrhalis	H. influenzae	E. coli	E. coli tolC
24	Cl	(structure)	-1.1	0.13	0.058	4.3	0.022	4	>64	>64	>64	>64	>64	>64
25	Br	(structure)	-1.0	0.30	0.068	4.8	0.053	4.6	>9	>9	-	>9	>9	>9
26	(structure)	(structure)	-2.1	-	-	-	0.15	>64	>64	>64	-	>64	>64	>64
27	(structure)	(structure)	-0.82	0.32	0.24	11	0.31	>9	>9	>9	>9	>9	>9	>9
28	(structure)	(structure)	-1.5	0.27	0.30	10	0.31	>64	>64	>64	>64	>64	>64	>64
29	(structure)	(structure)	-0.31	0.060	0.096	2.0	0.17	4.5	>64	>64	>64	>64	>64	36
30	(structure)	(structure)	0.12	0.030	0.012	2.3	0.072	0.66	>64	>64	43	43	>64	11
31	(structure)	(structure)	-0.62	<0.01	<0.01	0.51	<0.01	2.0	>64	>64	64	>64	>64	16
32	(structure)	(structure)	2.0	<0.01	0.017	0.96	0.012	0.09	2.7	1.4	0.7	5.5	>64	1.6
33	(structure)	(structure)	-	<0.01	<0.01	0.94	<0.01	2.8	>64	44	44	>64	>64	22
34	(structure)	(structure)	0.73	<0.01	<0.01	0.36	<0.01	0.05	3.1	6.1	1.6	12	>64	0.8

[a]Sau, Eco, and Spn indicate the enzymes from *S. aureus*, *E. coli*, and *S. pneumoniae*, respectively. [b]Bacterial strains are described in experimental procedures. [c]Methicillin sensitive *S. aureus*. [d]Methicillin resistant, quinolone resistant.
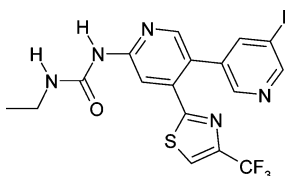
basis of this initial survey, ethyl-pyridylurea fragment **6** was chosen as the most promising starting point for further elaboration.

Inhibitory potency for compounds **14−41** was determined using two DNA gyrase and two topoisomerase IV isozymes (Table 1). The isozymes developed for assays in this investigation included DNA gyrase and topoisomerase IV from *E. coli*, DNA gyrase from *S. aureus*, and topoisomerase IV from *Streptococcus pneumoniae*. All compounds were also tested for antibacterial activities (defined by MIC, the minimum inhibitory concentration that afforded no visible growth in culture media) using seven bacterial strains from five bacterial species (Tables 1, 2, and 3). Results from the two *E. coli* topoisomerase assays allowed for correlation with the MIC values from two *E. coli* strains, a wild-type and a *tolC*⁻ efflux pump deficient strain.[39] MIC values were generally above the concentrations tested against the wild-type *E. coli* strain despite reaching low nanomolar potencies against the *E. coli* DNA gyrase. However, in the absence of efflux with the *tolC*⁻ stain, MIC values were improved, providing the hypothesis that low cellular accumulation of the compound prevented engagement of the target in the wild-type strains. In contrast, growth of the fastidious Gram-negative pathogens *Haemophilus influenzae* and *Moraxella catarrhalis* proved more susceptible to the series of compounds, perhaps due to higher membrane permeability. Activity against the *S. aureus* GyrB could be correlated with two *S. aureus* strains, a methicillin susceptible (MSSA) strain and a methicillin-resistant, quinolone-resistant (MRQR) strain. The *S. pneumoniae* ParE isozyme assay enabled correlation with

MIC data and, importantly, allowed exploration of structure−activity hypotheses when combined with the crystal structures of the ATPase domain of *S. pneumoniae* ParE. In general, relative inhibition by the compounds against the various isozymes showed good correlations, with the best inhibitors versus the *S. aureus* GyrB isozyme displaying better IC$_{50}$ values against the other three isozymes. It is perhaps better to consider relative rather than absolute IC$_{50}$ against the isozymes as the ATPase assays might not directly reflect the effect of inhibition of the biological topoisomerase function in cells.

All the compounds of Table 1 displayed improved potency against *S. aureus* GyrB ATPase relative to **6**. This includes the unsubstituted pyridine ring of compound **15**, which increased potency 12-fold over **6**. Modeling suggests that this pyridine substituent is coplanar with the scaffold's core pyridine ring and forms a π-interaction with the protein surface created by a flat edge-to-edge salt bridge between the binding pocket carboxylate of Glu58 and the guanidine of Arg84 (see below). The pyridine ring could be positioned to receive a hydrogen bond to Arg144 (see below) similar to the pyridine ring of **1**. The side chain of Arg144 is quite flexible, lacking a clear anchoring hydrogen bonding array or salt bridge association of the guanidine within the enzyme, and is thus able to adjust to the various inhibitors. Potency was improved versus all four isozymes (as much as 3-fold) for **19** relative to **15**, reflecting the addition of a carboxylate substituent potentially in proximity to Arg144. Other aromatic rings served well to position a carboxylate that maintained or improved enzyme inhibition, including the phenyl rings of **17** and **18**, the

Table 3. Influence of Bipyridyl Substituent on Isozyme Inhibition and MIC Values

Cmpd	R	logD	Sau[a] GyrB IC$_{50}$ (μM)	Eco GyrB IC$_{50}$ (μM)	Eco ParE IC$_{50}$ (μM)	Spn ParE IC$_{50}$ (μM)	MIC (μg/ml)[b]						
							S. pneumoniae	MSSA[c] S. aureus	MRQR[d] S. aureus	M. catarrhalis	H. influenzae	E. coli	E. coli tolC[-]
31	-CO$_2$H	-0.62	<0.01	<0.01	0.51	<0.01	2.0	>64	>64	64	>64	>64	16
32	-CONH$_2$	2.0	<0.01	0.017	0.96	0.012	0.09	2.7	1.4	0.7	5.5	>64	1.6
35	(oxadiazolone)	2.0	<0.01	<0.01	0.23	<0.01	0.05	0.04	0.06	0.04	0.69	>64	0.15
36	(methyl-oxadiazole)	2.4	<0.01	<0.01	0.51	0.015	0.05	0.19	0.26	0.37	33	>64	0.26
37	(methyl-oxadiazole)	3.4	0.052	<0.01	1.4	0.025	<0.095	0.37	0.19	0.74	>64	>64	0.74
38	(dimethyl-isoxazole)	3.5	0.30	0.068	4.8	0.053	4.6	>9	>9	-	>9	>9	>9
39	-CN	2.8	<0.01	<0.01	1.1	<0.01	<0.084	0.33	0.23	0.33	21	>64	0.33
40	(methyl-tetrazole)	-0.38	<0.01	<0.01	0.26	<0.01	1.4	>64	>64	>64	>64	>64	23
41	(amidoxime)	2.2	0.073	0.032	2.0	0.021	<0.01	0.36	0.72	0.18	1.4	>64	0.18
42	(methyl-oxadiazolone)	0.28	0.014	<0.01	1.5	0.011	0.74	48	48	24	>64	>64	12

[a]Sau, Eco, and Spn indicate the enzymes from *S. aureus*, *E. coli*, and *S. pneumoniae*, respectively. [b]Bacterial strains are described in experimental procedures. [c]Methicillin sensitive *S. aureus*. [d]Methicillin resistant, quinolone resistant.

thiazoles of **16** and **20**, and the benzthiazole of **21**. Extension to a carboxylate with the phenyl ether of **14** decreased potency, perhaps due to increased conformational flexibility relative to the directly bonded aromatic rings and disfavored coplanarity with the pyridine ring necessary to direct the carboxylate for the interaction with the arginine. Nonetheless, the phenylcarboxylate substituent of **14** improved potency 3-fold over **6**. Meshing with the apparent mobility of the Arg144 side chain, there were preferences for potency depending on the position of the carboxylate. The 1,3 orientation between a carboxylate and the point of attachment to the scaffold for thiazole **20** shows a 10-fold higher potency against *S. aureus* GyrB relative to the 1,3 orientation of the isomeric **16**. Extending the carboxylate further outward from the pyridylurea pharmacophore with the benzthiazole of **21** improved potency 3−4-fold over **20**, depending on the isozyme. Many of the compounds in Table 1 showed higher ligand efficiencies (the ligand efficiencies ranged from 0.52 for **14** to 0.76 for **20** using the *S. aureus* IC$_{50}$ data) than **6**. Furthermore, measurable MIC values versus *S. pneumoniae*, *M. catarrhalis*, and *H. influenzae* indicated that the higher inhibition translated into antibacterial activity allowing for rational structure−activity correlations.

Considerable improvement in potency was further achieved by positioning substituents at the pyridylurea 4-position (Table 2). Modeling showed that substituents at this 4-position extend into the ATP binding pocket toward an open region where the ATP ribose ring is situated. This region is bounded by a loop

that is ordered in the dimeric structures of the 43 kDa GyrB domain bound to an ATP analogue[37] and is disordered in monomeric 24 kDa GyrB and ParE-inhibitor complexes. The smaller chlorine and bromine substituents of compounds **24** and **25** improved potency 6−24-fold depending on the isozyme. Compounds **27** and **28**, with pyridine substituents on the 4-position, also displayed improved potency relative to hydrogen (compound **19**), albeit the improvement was less than that of the halogen substituents. Compound **29** with the phenyl substituent increased potency 10-fold or more relative to **19** versus three of the isozymes and 2-fold versus the fourth. Notably, the thiazole substituents of **30−34** afforded further potency improvements that can be attributed to positioning a lipophilic group (*t*-butyl for **30** and CF$_3$ for **31−34**) toward complementary lipophilic regions of GyrB and ParE (see below).

Higher solubility is a critical factor for the development of a therapeutic molecule to enable formulation development and maintain efficacious levels of the drug in vivo. Compounds with an ionizable carboxylic acid substituent consistently imparted higher solubility; however, the carboxamide analogues displayed superior antibacterial activity compared to those with acid substituents (e.g., compare **22** to **20**, Table 1 and **32** to **31**, Table 3). Therefore, achieving sufficient solubility for this drug scaffold was required while also improving antibacterial activity either by increasing inhibitory potency or improving bacterial membrane permeability. That carboxamides and carboxylic
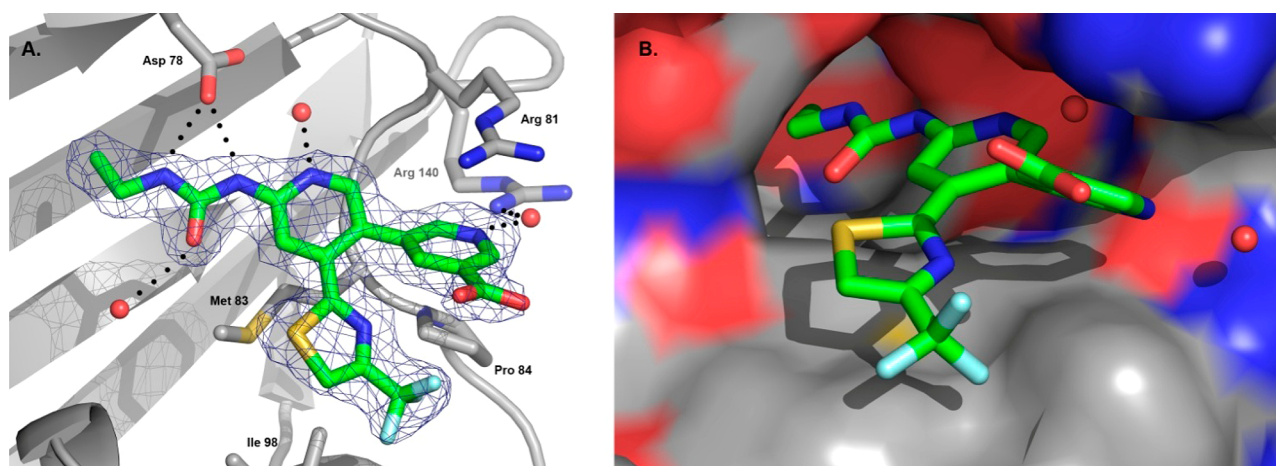
Figure 4. (A) **31** in binding site of *S. pneumoniae* ParE ATPase domain. Hydrogen bonds are shown as dotted lines. $2F_o - F_c$ density has been contoured to 1.0σ. The urea pyridylurea core is oriented in the binding pocket to form a bifurcated hydrogen bond between the urea and Asp78. A crystallographic water bridges Asp78 to the pyridine nitrogen. Another crystallographic water bridges Arg140 to the second pyridine nitrogen. The CF$_3$-thiazole abuts a hydrophobic surface formed by Met83, Ile98, and Pro84. (B) Surface representation of the binding site of **31**. The pyridine substituent π-stacks with Arg81(blue surface, upper right), and the carboxylate is oriented away from Arg140 (blue surface, right).

acids show comparable enzyme inhibition presumably reflects a trade-off for greater enthalpic contribution to binding with ionized acids and greater entropic contribution to binding with neutral amides. In essence, there is a greater desolvation penalty for taking the carboxylate from the aqueous environment to the enzyme binding region for the interaction with the Arg144 guanidine. The dichotomy arises when analyzing antibacterial activity as the capability of charged acids to traverse the bacterial lipid bilayer is lower than neutral, more lipophilic compounds.[40,41] Hence, compounds **32** and **34** with higher log D displayed the better MIC values among compounds of similar inhibitor potencies in Table 3. The comparison of benzthiazoles **23** and **21** provides, perhaps, a counterexample to this, as antibacterial activity does not track well with either potency or lipophilicity in that the former performed worse than the latter, in particular against the *E. coli tolC⁻* strain. This is attributed to the low solubility of **23** (<1 μM), likely undermining reliable MIC measurement under the assay conditions. Higher lipophilicity generally favors membrane permeability and thus, antibacterial activity, but disfavors solubility crucial for achieving higher plasma concentrations in vivo and, as in the case with **23**, for achieving sufficient concentrations for even in vitro MIC assessments.

Indeed, the fact that there is not a direct correlation between GyrB/ParE enzyme inhibition and antibacterial activity can be attributed to a variety of reasons beyond the vagaries of compound membrane permeability and solubility. Considerable extrapolations have been made among the isozymes surveyed for correlations with MIC data from the different bacterial species. As mentioned, inhibitors of the GyrB ATPase activity are generally also inhibitors of ParE ATPase activity, and the relative role of each for inhibition in an enzyme assay and in the bacterial cytoplasm cannot easily be teased apart and might be better ascertained from resistance development studies and genomic analysis.[42] Enzyme inhibition is measured by ATPase activity coupled through detection of phosphate release in a Malachite Green assay, which is different from the physiologically relevant catalytic cycle with DNA that occurs inside the bacterial cell. Finally, the assays do not account for expression levels and regulatory mechanisms within the bacterial cell that are also important for translation to MIC.[43] Nonetheless, the

enzyme assays serve well to ascertain structure−activity relationships; for example, IC$_{50}$ values less than 50 μM against the *S. aureus* GyrB isozyme were necessary to afford MIC values less than 64 μg/mL versus the *S. aureus* strains.

The antibacterial mode-of-action of compound **32** was assessed by monitoring its influence on the incorporation of radioactive thymidine, uridine, leucine, and valine, acetic acid, and *N*-acetylglucoseamine into bacterial cells as indicators for DNA, RNA, protein, fatty acid, and peptidoglycan biosynthesis, respectively (see Table 5).[28,44] Two pathogens, *S. aureus* and *S. pneumoniae*, were surveyed, and the low IC$_{50}$ values recorded for thymidine incorporation indicate that the primary mode of action of these inhibitors is the preferential disruption of DNA synthesis, consistent with topoisomerase (GyrB and ParE) inhibition. The observed inhibition of RNA and protein syntheses, as measured by reduced uridine and amino acid incorporation, is believed to be a consequence of the inhibition of DNA synthesis rather than a secondary mode of action and was similarly observed for compound **1**.[45] However, the ciprofloxacin IC$_{50}$ values for metabolite incorporation for DNA synthesis was considerably more pronounced relative to the other metabolic processes despite the fact that this molecule also acts through inhibition of bacterial topoisomerases. This may be the consequence of faster killing kinetics observed for ciprofloxacin versus **32** (data not shown), triggering cell death before effects are seen for RNA and protein synthesis and may reflect the different mechanisms of topoisomerase inhibition for the two molecules. No effects were seen at the concentrations of **32** tested on peptidoglycan or fatty acid biosyntheses. Positive controls rifampicin, erythromycin, triclosan, and penicillin G showed the expected profiles for the inhibition of radiolabel precursor incorporation into RNA, protein, fatty acid, and cell wall biosyntheses, respectively (data not shown).

A 2.06 Å crystal structure of compound **31** with the 23 kDa N-terminal ATPase domain of the *S. pneumoniae* ParE topoisomerase IV isozyme was determined (Figure 4 and Table 8). The particular isozyme had proven robust for crystallography work, affording high resolution data with a variety of inhibitor complexes including 4EMV and 4EM7 in the Protein Data Bank.[26] The isozyme binding pocket further reflects the high degree amino acid sequence conservation

Table 4. PK Properties of Selected Compounds
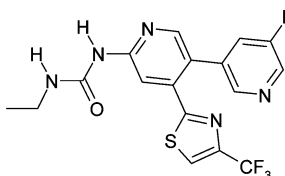
Cmpd	R	Solubility (μM)	Human ppb (%free)	pKa	Rat clearance (mL/min/kg)	Rat V_{ss} (L/kg)	Mouse clearance (mL/min/kg)	Mouse V_{ss} (L/kg)
31	$-CO_2H$	800	8.2	3.7	-	-	-	-
32	$-CONH_2$	26	36	-	120	1.5	-	-
35	(oxadiazolone)	19	4.4	6.6	36	0.66	74	2.6
36	(methyl-oxadiazole)	1	11	-	123	3.3		
37	(methyl-oxadiazole)	<1	6.3	-	100	11	-	1
38	(dimethyl-isoxazole)	6	4.5	-	-	-	-	-
39	$-CN$	7	5.9	-	110	3.4	-	-
40	(tetrazole)	240	14	3.7				
41	(amidoxime)	4	35		22			
42	(oxadiazolone)	830	1.1	5.4	360	3.5	-	-

across species and between DNA gyrase and topoisomerase IV.[46] Although the construct itself does not have ATPase activity displayed by the full ParE used for activity assays, the integrity of the inhibitor binding pocket was maintained. The structure showed that the pyridylurea pharmacophore of the molecule formed a bifurcated hydrogen bond with Asp78 (equivalent to Asp81 for *S. aureus* GyrB used for modeling work), which was, in turn, hydrogen-bonded to a structurally conserved water molecule similar to the diagram for **1** in Figure 1. The water molecule otherwise bridged the core pyridine nitrogen of **31** and Thr172 through hydrogen bonds. From the perspective of inhibitor design, this water molecule is tightly coordinated in this and other published structures and therefore would be difficult to displace. A second water molecule bridged the urea carbonyl to the side chain carboxamide of Asn51 and the hydroxyl of Ser124. The key hydrogen bond interactions with Asp78 and the two water molecules seen for **31** mimicked those made by adenine with ATP analogues bound to the enzyme.[37] In contrast, an X-ray structure determination of **2** with the *S. aureus* GyrB ATPase domain did not show the second water molecule, with the region being occupied by the dichloropyrrole moiety and a direct interaction being seen to Asn54 (*S. aureus* GyrB numbering, equivalent to Asn51 of *S. pneumoniae* ParE).[36]

The trifluoromethylthiazole substituent of **31** was positioned in the hydrophobic patch that forms part of the ribose binding pocket with the thiazole ring contacting Met83 and the trifluoromethyl group fitting snugly in a small pocket formed by the adjacent residues Pro84, Thr94, and Ile98, perhaps accounting for the potency enhancements. The 5-position pyridine substituent off the core pyridylurea formed a π-stacking interaction with Arg81 in line with what was considered in the compound design. Interestingly, the pyridine nitrogen engages the Arg140 (equivalent to Arg144 for *S. aureus* GyrB) through a bridging water molecule rather than through a salt bridge with the acid, which is oriented away from the arginine residue toward the solvent. This result is in contrast to the design hypothesis and inhibition data that would have predicted the carboxylate improving inhibitory potency. It also contrasts the structure solved for **1**, where the pyridine nitrogen makes a direct hydrogen bond to Arg144. It should be noted that the crystallization was carried out with the 226 residue N-terminal ATPase domain of the *S. pneumonia* ParE rather the entire 648 residue GyrB protein or a larger topoisomerase IV ParC−ParE complex, which could misrepresent the physiologically relevant binding orientation. Nonetheless, among the structures that have been solved, although the hydrogen bond interactions with arginine have been deemed

important for improving inhibitor potencies, there appears to be a measure of plasticity for the arginine side chain conformation.

As suggested earlier, compounds should have sufficiently high solubility and high antibacterial activity as two important components toward the design of a viable drug. To this end, the compounds of Table 3 incorporated alternative functionality to the acid of **31** that had low antibacterial activity despite high topoisomerase inhibitory potency and the amide of **32** that had high antibacterial activity but moderate solubility (see Table 4). Inhibitory potencies of **35–40** versus the four topoisomerase isozymes were among the highest reported herein, albeit the weak antibacterial activity of **39** and **42** with the more acidic acid isosteres paralleled the properties of **31**. Indeed, a clear correlation emerged in that R groups with higher acidity (Table 4) led to weaker antibacterial activities despite inhibitory potencies that were comparably high. Compounds **31**, **35**, **40**, and **42** displayed potent inhibition across the four topoisomerase isozymes but were varied in acidity displaying correspondingly varied MIC values; for example, the least acidic compound **35** having a measured pK_a of 6.6 afforded the highest antibacterial activity. Figure 5 illustrates this correlation
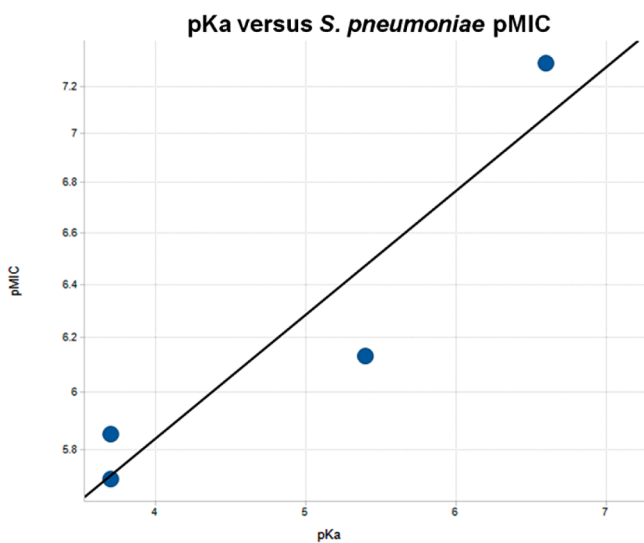

Figure 5. Correlation between antibacterial activity and pK_a.

in a plot of *S. pneumoniae* pMIC versus pK_a for the four compounds. Although higher acidity improved solubility, multiple factors (physical properties, antibacterial activity, and in vivo kinetics) must be balanced to design potent and effective drug candidates for clinical use. Compounds **36**, **37**, and **39** showed similar properties to **32** in that antibacterial activity was high but solubility was low. Compound **41** showed considerably weaker intrinsic potency and antibacterial activity relative to **35** but better antibacterial activity relative to the more acidic compounds **36**, **37**, and **39**. Overall, compounds **32** and **35**, though of moderate solubility, had the balance of properties necessary for demonstrating in vivo activity. Because the concentration of unbound compound in blood must be sufficiently high and sustained to demonstrate efficacy in animal disease models, compound **35** with the lower clearance in the rat (Table 4) was selected for efficacy experiments in an in vivo disease model (see below).

An X-ray crystal structure of **35** bound to the *S. pneumoniae* ParE was determined (Figure 6). As expected, most of the
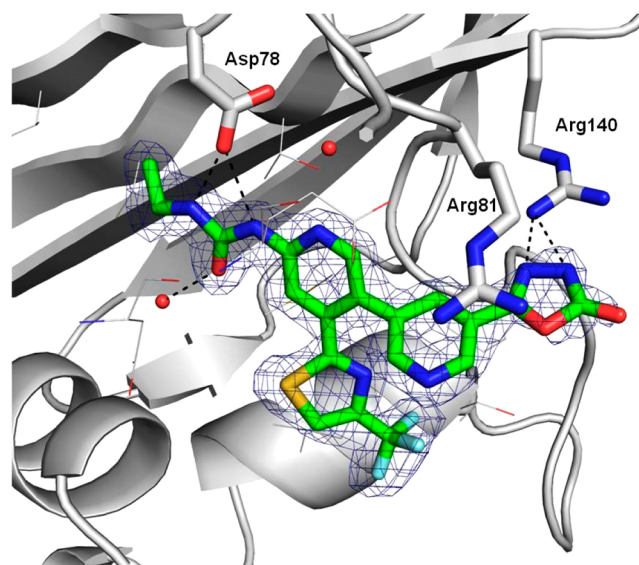

Figure 6. X-ray crystal structure of **35** in *S. pneumoniae* ParE. The hydrogen bonding array around Asp78 is maintained relative to **32** (Figure 4). The pyridyl-oxadiazolone substituent π-stacks with Arg81; the oxadiazolone forms a salt bridge with Arg140.

interactions between the **35** and the protein paralleled those seen for **31**. However, unlike the strong acid carboxylate of compound **31**, a clear interaction was seen between the weakly acidic oxadiazolone moiety and the Arg140 guanidinium. It is notable that Arg81 (which stacks over the π-cloud of the distal pyridine rings of both **31** and **35**) and Arg140 lie outside the ATP binding region but are well conserved due to their contributions to protein–protein interactions critical to stabilizing the GyrB and ParE dimers.[37,47] Although these residues are not important for substrate binding, they nonetheless play important roles for the enzyme and therefore should not be candidates for nonsimilar mutation leading to drug resistance. Binding interactions with these arginine residues have been exploited in other classes of GyrB inhibitors.[25–32,34–36,48–50]

For compounds active versus *S. aureus* in Tables 2 and 3, it is noteworthy that the MRQR strain was nearly equally affected as the MSSA strain. This MRQR strain carries a SCC*mec* type II resistant allele imparting methicillin resistance[51] and an S85P GyrA and S80Y ParC mutation imparting reduced susceptibility to fluoroquinolone DNA gyrase inhibitors. In contrast, the fluoroquinolone levofloxacin showed large differences between the strains with MIC values of 0.13 and 4 μg/mL for the MSSA and MRQR *S. aureus* strains, respectively. Similarly, clinical strains of *S. pneumoniae* with reduced susceptibility to levofloxacin were equally susceptible to compound **35** compared with the wild-type strain (data not shown, however see Table 6 for nonclinical strains). These results were expected because the mode of DNA gyrase inhibition of ATP-competitive compounds differs from that of fluoroquinolones, with the latter binding to cleaved DNA at the interface between GyrA and GyrB[52] as well as ParC and ParE.[53] As a positive control, novobiocin behaved similarly to **35** in that MIC values were not affected by the fluoroquinolone resistant strains nor were they affected by nontopoisomerase binding antibacterials such as tetracycline.[54] These data bode well for this series of DNA gyrase inhibiting compounds in that susceptibility in the

Table 5. Inhibition of Radioactive Precursor Incorporation into Bacterial Cells over 1 h

	S. aureus IC$_{50}$ (μM)			*S. pneumoniae* IC$_{50}$ (μM)	
radiolabel precursor	32	ciprofloxacin	radiolabel precursor	32	ciprofloxacin
^{3}H-thymidine	1.6	3.9	^{3}H- thymidine	0.46	28
^{3}H-uridine	6.9	>195	^{3}H-uridine	0.83	>200
^{14}C-leucine	8.8	>174	^{14}C-leucine	0.86	110
^{14}C-valine	31	>195	^{14}C-valine	1.2	>200
^{14}C-acetic acid	>200	>195	^{14}C-acetic acid	>20	>200
^{14}C-*N*-acetyl glucosamine	>200	>195	^{14}C-*N*-acet-glucosamine	>20	>200

Table 6. MICs (μg/mL) versus *S. pneumoniae* Strains with Mutations in DNA Gyrase and Topoisomerase IV

compd	wild-type	GyrB T172A ParE none	GyrB K143I ParE none	GyrB none ParE T172A	GyrB T172A ParE T172A	GyrB K143A ParE T172A	GyrA S81F ParC S79F	GyrA S81Y ParC S79F	GyrA S81F ParC S79Y
35	0.0025	0.01 (4×)	0.01 (4×)	0.01 (4×)	0.02 (8×)	0.04 (16×)	0.0025	0.0025	0.0025
novobiocin	0.5	2 (8×)	1 (4×)	0.25 (1×)	4 (16×)	4 (16×)	0.25	0.25	0.25
levofloxacin	1	0.5	1	1	0.5	0.5	16 (16×)	16 (16×)	32 (32×)
tetracycline	0.25	0.25	0.25	0.25	0.25	0.25	0.13	0.25	0.13

clinic should be maintained versus bacteria with pre-existing drug resistance due to DNA gyrase mutations.

The importance of several interactions observed in the cocrystal structure was investigated by creating point mutations in the *gyrB* and *parE* genes of *S. pneumoniae*. The amino acids selected for this study (see Table 6) were derived from those investigated for other ATP competitive topoisomerase inhibitors.[28,42,45,55] The two threonine residues, Thr172 from each of GyrB and ParE, lie in hydrogen bonding distance to the water molecule otherwise coordinated with Asp78 in the adenine binding pocket. The GyrB residue Lys143, analogous to the ParE Arg140, is presumed to interact similarly with the acidic oxadiazolone moiety of 35 as seen in the ParE complex structure. Single point mutations T172A in GyrB and ParE and K143I in GyrB resulted in a 4-fold elevation of MIC for 35 when compared to the MIC for the parent strain, whereas combinations of these mutations in both genes resulted in an 8−16-fold elevation in MIC. In contrast, results for novobiocin against these mutants were somewhat different, where only the GyrB mutants displayed debilitated MIC (4−16-fold) while the ParE single mutant T172A showed no increase in MIC. These results parallel those reported for aminobenzimidazole class of GyrB inhibitors such as 1[42] and similarly indicate that the dual mode-of-action for 35 is more balanced than that for novobiocin and that the interactions influencing ATPase inhibition for each of the two topoisomerases can vary depending on the scaffold.

S. pneumoniae strains were also made in which mutations in *gyrA* and *parC* were constructed to confer resistance to fluoroquinolone drugs such as levofloxacin (Table 6).[56] Compound 35 and novobiocin maintained potent MIC values in line with data for the wild-type parent strain, while the MIC values were elevated, appropriately, for levofloxacin. None of the GyrB/ParE mutations in Table 6 are necessarily relevant to what might be seen clinically, but they do confirm that the binding site delineated by X-ray crystallography as being relevant to antibacterial activity and that the mode-of-action involving both DNA gyrase and topoisomerase IV for *S. pneumoniae* that is distinct from that for fluoroquinolones.

As a means to assess the risk of future resistance development, the frequency of spontaneous resistance was measured with increasing concentrations of 35 in *S. aureus* (MSSA) cultures (Table 7). The frequency of spontaneous

Table 7. Frequency of Spontaneous Resistance for 35 against *S. aureus* and MICs for Resulting Mutants

[compound] μg/mL	fold MIC	resistance frequency	MIC shift[a]
0.05	1×	1.1×10^{-9}	16×
0.1	2×	1.3×10^{-9}	16×
0.2	4×	3.0×10^{-10}	16×

[a]Elevation of MIC for selected mutants relative to parent strain.

resistance of approximately 1×10^{-9} for 35 is low, suggesting that development of resistance should not be rapid. MIC values for the resulting mutant strains were elevated 16-fold relative to the wild-type parent strain. DNA sequencing of the genes encoding the topoisomerase subunits (*gyrA*, *gyrB*, *parC*, and *parE*) from two of these resistant mutant strains revealed the same point mutation in the *gyrB* gene when compared to sequences obtained from the sensitive parent strain. This mutation resulted in a single amino acid change in GyrB, T173N, which is the same amino acid as Thr172 mutated in the engineered *S. pneumoniae* strains described above. Similar mutations, generated in vitro, have been reported to be associated with resistance to several other chemical series that target the ATP binding pocket of DNA gyrase.[28,45,55] Although these mutants can be generated in the laboratory, similar mutations in *gyrB* have not been observed in any clinical isolates of *S. aureus* or *S. pneumoniae* sequenced in house (data not shown) or reported in the literature to date, presumably due to the lack of ATPase inhibitors currently in clinical use.

Compound 35 was evaluated in vivo against *S. aureus* in a neutropenic mouse thigh infection model.[57] Thigh infection was established with *S. aureus* at 1×10^5 CFU (colony-forming units)/thigh in mice previously rendered neutropenic by treatment with cyclophosphamide, as described previously.[58] Dosing of 35, or vehicle control, by intraperitoneal (ip) injection commenced 2 h post infection and a second, equal dose was administered 12 hours after the first resulting in a total daily doses of 80, 120, 160, 200, and 300 mg/kg. Activity was quantified by viable counts of thigh homogenates 24 h after start of the treatment and is presented in Figure 7 as mean log CFU/g thigh tissue (± standard error) for each group of mice. Compound 35 was found to be efficacious against *S. aureus* in this model, causing a dose-dependent decrease in viable bacterial counts in the thigh. A dose of 300 mg/kg resulted
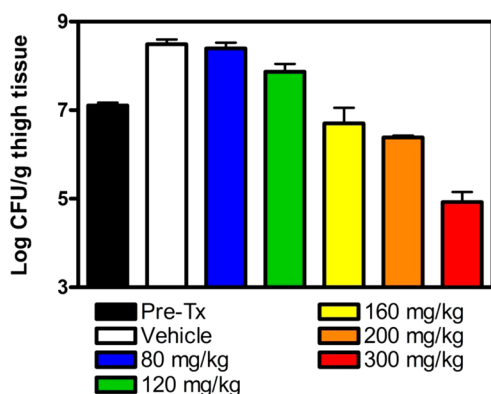
Figure 7. Efficacy of compound **35** in a 24 h *S. aureus* thigh infection model in neutropenic mice. Bars from left to right show the number of *S. aureus* colony forming units (CFU) recovered from thighs of mice treated with 0−300 mg/kg of compound **35** administered by ip injection at 0 and 12 h. Total doses are shown. Error bars represent standard error in the CFU measurements.

in the maximum response, a 3000-fold reduction in bacterial burden relative to the vehicle control. The ED_{50} for **35** in this model was estimated to be 200 mg/kg.

CONCLUSIONS

In summary, a series of urea pyridine fragments designed based on the crystal structure of topoisomerase ATPase domains with known inhibitors generated a valuable starting point for elaboration into compounds with antibacterial activity. This fragment-to-hit-to-lead sequence has spawned a robust optimization program that will be reported in subsequent publications and has been exemplified in the public domain as patent applications.[59−65] Lead compounds were developed to engineer a higher aqueous solubility to facilitate further development, hence, the emphasis on incorporating the ionizable carboxylic acid and acid isoster moieties designed to serve the dual roles of increasing solubility and interacting with the binding domain arginine residue (Arg140, *S. pneumoniae* ParE). The cocrystal structures of compounds **31** and **35** offer support for many of the design hypotheses including the incorporation of binding interactions with an aspartate residue associated with binding to the adenine portion of ATP and with the arginine that lines the inhibitor pocket distal to the ATP binding domain. That said, there remains a measure of ambiguity for the importance of the carboxylate of **31** in the interaction with Arg140 in that the X-ray derived crystallographic model showed the distal pyridine nitrogen oriented toward the Arg140 with the *S. pneumoniae* ParE isozyme rather than the carboxylate. By contrast, the oxadiazolone of **35** did indeed bridge to Arg140 as anticipated by design. Building substituents on the urea-pyridine 4-postion was central for a notable improvement in inhibitory potency by occupying a hydrophilic region of the enzyme with a lipophilic CF_3 group. Overall, potent inhibition across four topoisomerase isozymes from three bacterial species was realized. Importantly, inhibition of bacterial growth was demonstrated via a mode-of-action that involves both DNA gyrase and topoisomerase IV, which serves as the key criterion to continue optimization work and to improve properties (e.g., antibacterial potency, pharmacokinetics, solubility) that would support the demonstration of efficacy in animal models and utility in the clinic. Ultimately, efficacy in a murine disease model was demon-

strated with ip administration of **35**. For translation to utility in the clinic, further analogue optimization work from the promising lead compounds shown here is needed to afford more soluble compounds that maintain potent antibacterial activity and improve in vivo PK properties. The structural features correlating with activity for these pyridylureas differentiates from those for compounds **1** or **2** and offer alternative motifs to design and develop antibacterial agents targeting bacterial topoisomerase binding targets.

EXPERIMENTAL PROCEDURES

General Considerations. All of the solvents and reagents used were obtained commercially and used as such unless noted otherwise. ^{1}H NMR spectra were recorded in $CDCl_3$ or DMSO-d_6 solutions at 300 K using a Bruker 300 Ultrashield 300 MHz instrument. Chemical shifts are reported as parts per million relative to the reference TMS (0.00). ^{13}C NMR spectra were recorded in DMSO-d_6 solutions at 300 K and 126 MHz using a Bruker DRX-500 500 MHz instrument with a QNP cryoprobe or at 101 MHz using a Bruker 300 Ultrashield 300 MHz instrument. Chemical shifts are reported as parts per million relative to the reference TMS (0.00). High-resolution mass spectra (HRMS) were obtained using a hybrid quadrupole time-of-flight mass spectrometer (microTOFq II, Bruker Daltonics) in ESI$^+$ mode. Silica gel chromatographies were performed on an ISCO Combiflash Companion instrument using ISCO RediSep flash cartridges (particle size: 35−70 μm) or Silacycle SiliaSep flash cartridges (particle size: 40−63 μm). Preparative reverse phase HPLC was carried out using YMC Pack ODS-AQ (100 mm × 20 mm ID, S-5 μ particle size, 12 nm pore size) on Agilent instruments. Mass spectroscopy was performed using a Waters ZQ mass spectrometer (for ESP) connected to a Agilent 1100 HPLC instrument. All compounds tested possessed a purity of ≥95%. Compounds **4** and **12** were purchased from chemical supply houses. Compounds for oral and iv dosing in mice were formulated in 25% PEG/water and 4:4:2 dimethylacetamide−PEG400−water, respectively. Compounds for iv and ip dosing in rats were formulated in 70% PEG/30% saline (13% HP cyclodextrin). Wistar Han rats were used for pharmacokinetic studies and were obtained from Charles River Laboratories (Raleigh, NC). CD-1 mice were obtained from Charles River Laboratories (Kingston, NY) for efficacy studies. All animals were housed and acclimated in the animal facility on site before each study. All experimental procedures were conducted in accordance with protocols approved by the Institutional Animal Care and Use Committee.

1-(1H-Benzimidazol-2-yl)-3-ethyl-urea (3). A mixture of 1*H*-benzo[*d*]imidazol-2-amine (300 mg, 2.25 mmol) and ethylisocyanate (0.36 mL, 4.5 mmol) in chloroform (4 mL) was heated at 100 °C in a microwave reactor for 2 h. LC-MS shows two materials suggesting a mixture of acylation products. Solvent was removed from the mixture, and the residue was purified by reverse phase HPLC (5−79% 0.1% formic acid in water and acetonitrile). The first eluting component was consistent with the title compound isolated as a solid (137 mg, 30% yield). ^{1}H NMR (DMSO-d_6) δ 11.5 (s, br, 1H), 9.6 (s, br, 1H), 7.3−7.4 (m,3H), 6.9−7.0 (m, 2H), 3.2 (pentet, 2H), 1.1 (s, 3H). ^{13}C NMR (DMSO-d_6, 126 MHz) δ 154.1, 148.3, 120.4, 34.1, 15.3. LC-MS purity 100%. MS (ESI) m/z 275 [M + H]$^+$. HRMS [M + H]$^+$ = 205.1090 (theoretical 205.1084).

Compounds **8** and **13** were synthesized similarly as compound **3** from the starting aminoheterocycle and the appropriate isocyanate.

1-Propyl-3-(2-pyridyl)urea (8). Solid, 500 mg (87%) using 2-aminopyridine (300 mg) and *n*-propylisocyanate (0.45 mL). ^{1}H NMR (DMSO-d_6) δ 9.6 (s, 1H), 9.0 (s, 1H), 8.6 (d, 2H), 7.0 (t, 1H), 3.25 (pentet, 2H), 1.1 (t, 3H). ^{13}C NMR (DMSO-d_6, 126 MHz) δ 154.7, 153.5, 146.6, 138.1, 116.6, 111.5, 40.7, 22.9, 11.4. LC-MS purity 100%. MS (ESI) m/z 167 [M + H]$^+$. HRMS [M + H]$^+$ = 167.0921 (theoretical 167.0927).

1-Ethyl-3-(2-pyrimidin-2-yl)urea (13). Solid, 120 mg (32%) using 2-aminopyrimidine (320 mg) and ethylisocyanate (0.36 mL). ^{1}H NMR (CDCl$_3$) δ 9.35 (s, br, 1H), 8.1−8.3(m, 1H), 7.6 (ddd, 1H), 6.9

(m, 1H), 6.8 (d, 1H), 3.4 (dt, 2H), 1.7 (m, 2H), 1.0 (t, 3H). ^{13}C NMR (DMSO-d_6, 126 MHz) δ 158.2, 158.0, 153.8, 114.4, 34.0, 15.3. LC-MS purity 100%. MS (ESI) m/z 180 [M + H]$^+$. HRMS [M + H]$^+$ = 180.1136 (theoretical 180.1131).

1-Ethyl-3-(2-pyridyl)urea (6). A mixture of 2-(phenoxycarbonyla-mino)-pyridine^{66} (100 mg, 0.47 mmol) and 3 mL (6 mmol) of 2N ethylamine in THF was heated at 80 °C for 30 min in a microwave reactor. Solvent was removed, and the residue was purified by silica gel chromatography (100% CH$_2$Cl$_2$ followed by gradient elution to 80% EtOAc in CH$_2$Cl$_2$) to afford 70 mg (90%) of the title compound as a solid. ^{1}H NMR (DMSO-d_6) δ 9.15 (s, 1H), 8.2 (m, 2H), 7.6 (t, 1H), 7.3 (d, 1H), 6.9 (m, 1H), 3.2 (q, 3H), 1.1 (t, 3H). ^{13}C NMR (DMSO-d_6, 126 MHz) δ 154.6, 153.5, 146.6, 136.5, 138.1, 116.6, 111.5, 33.8, 15.4. LC-MS purity 99%; MS (ESI) m/z 166 [M + H]$^+$. HRMS [M + H]$^+$ = 166.0982 (theoretical 166.0982).

Compounds **5**, **7**, and **9−11** were synthesized similarly as compound **6** from 75 mg of 2-(phenoxycarbonylamino)-pyridine.

1-Methyl-3-(2-pyridyl)urea (5). Solid, 46 mg (65%) using 2N methylamine in THF. ^{1}H NMR (DMSO-d_6) δ 9.2 (s, 1H), 8.1 (m, 2H), 7.7 (t, 1H), 7.3 (d, 1H), 6.9 (t, 1H), 2.7 (s, 3H). LC-MS purity 100%. ^{13}C NMR (DMSO-d_6, 126 MHz) δ 155.3, 153.5, 146.6, 138.1, 116.6, 111.4, 25.9. MS (ESI) m/z 152 [M + H]$^+$. HRMS [M + H]$^+$ = 152.0823 (theoretical 152.0826).

1-Prop-2-ynyl-3-(2-pyridyl)urea (7). Solid, 48 mg (78%) using diethylamine. ^{1}H NMR (DMSO-d_6) δ 9.35 (s, 1H), 8.5 (s, 1H), 8.2 (d, 1H), 7.7 (t, 1H), 7.3 (d, 1H), 6.95 (t, 1H) 4.0 (dd, 1H), 3.1 (t, 1H). ^{13}C NMR (DMSO-d_6, 126 MHz) δ 154.4, 153.1, 146.7, 138.3, 117.0, 111.6, 81.7, 73.0, 28.5. LC-MS purity 100%. MS (ESI) m/z 176 [M + H]$^+$. HRMS [M + H]$^+$ = 176.0823 (theoretical 176.0826).

1-Cyclopropyl-3-(2-pyridyl)urea (9). Solid, 41 mg (66%) using cyclopropylamine,. ^{1}H NMR (DMSO-d_6) δ 9.1 (s, 1H), 8.1 (s, 2H), 7.7 (m, 1H), 7.3 (m, 1H), 6.8 (m, 1H), 2.6 (m, 1H), 0.7 (m, 2H), 0.4 (m, 2H). LC-MS purity 100% MS (ESI) m/z 178 [M + H]$^+$. HRMS [M + H]$^+$ = 178.0984 (theoretical 178.0982).

1-(2-Pyridyl)-3-(2,2,2-trifluoroethyl)urea (10). Solid, 45 mg (59%) using trifluoroethylamine. ^{1}H NMR (DMSO-d_6) δ 9.5 (s, 1H), 8.7 (s, 1H), 8.2 (d, 1H), 7.7 (m, 1H), 7.4 (m, 1H), 7.0 (m, 1H), 4.0 (m, 2H). ^{13}C NMR (DMSO-d_6, 126 MHz) δ 154.6, 152.9, 146.7, 138.5, 125.0, 117.4, 111.8, 39.5 (overlaps DMSO resonace). LC-MS purity 100%. MS (ESI) m/z 220 [M + H]$^+$. HRMS [M + H]$^+$ = 220.0702, (theoretical 220.0699).

1,1-Diethyl-3-(2-pyridyl)urea (11). Oil, 40 mg (59%) using diethylamine. ^{1}H NMR (DMSO-d_6) δ 8.6 (s, 1H), 8.2 (d, 1H), 7.85 (d, 1H), 7.7 (t, 1H), 7.0 (t, 1H), 3.4 (q, 4H), 1.1 (t, 6H). ^{13}C NMR (DMSO-d_6, 126 MHz) δ 155.5, 152.0, 147.3, 137.4, 117.6, 113.3, 40.6, 13.8. LC-MS purity 100%. MS (ESI) m/z 194 [M + H]$^+$. HRMS = 194.1296 (theoretical 194.1295).

Methyl 3-(6-Nitropyridin-3-yloxy)benzoate. NaH (0.095 g, 2.36 mmol, 60% dispersion in oil) was added to a solution of the methyl 3-hydroxybenzoate (0.36 mg, 2.36 mmol) in DMF (4 mL) at room temperature with gas evolution and formation of a light-yellow solution. 5-Bromo-2-nitropyridine (0.40 mg, 1.97 mmol) was added, turning the reaction mixture into a brown solution. The reaction mixture was heated at 60 °C for 1 h before being partitioned between water and EtOAc. The layers were separated and the organic layer was washed with water and dried over MgSO$_4$. The EtOAc was filtered and concentrated to give a brown oil that was purified by chromatography on silica gel (hexanes/EtOAc) to give 0.32 g of the title compound, which was used subsequently without further purification. MS (ESI) m/z 275 [M + H]$^+$.

Methyl 3-(6-Aminopyridin-3-yloxy)benzoate (43). A mixture of 10% palladium on carbon (30 mg) in methanol (5 mL) and methyl 3-(6-nitropyridin-3-yloxy)benzoate (320 mg, 1.17 mmol) was degassed with nitrogen and left under a hydrogen atmosphere overnight. The reaction mixture was filtered, and the filtrate was concentrated to give 230 mg of a clear oil consistent with the title compound, which was used subsequently without further purification. MS (ESI) m/z 245 [M + H]$^+$.

3-(6-(3-Ethylureido)pyridin-3-yloxy)benzoate. A solution of meth-yl 3-(6-aminopyridin-3-yloxy)benzoate **42** (0.23 mg) and ethyl-

isocyanate (0.082 mL) in chloroform (5 mL) was heated in a microwave reactor at 110 °C for 1 h. Solvent was removed, and the residue was chromatographed on silica gel (gradient elution with 2% MeOH in CH$_2$Cl$_2$ to 10% MeOH in CH$_2$Cl$_2$) to give 0.12 g (42%) of the title compound as a white solid. ^{1}H NMR (DMSO-d_6) δ 1.07 (t, 3H), 3.16−3.22 (m, 2H), 3.82 (s, 3H), 7.25−7.28 (m, 1H), 7.36 (s, 1H), 7.45−7.55 (m, 3H), 7.60−7.71 (m, 2H), 8.06 (s, 1H), 9.20 (s, 1H). MS (ESI) m/z 316 [M + H]$^+$.

N-Ethyl-N'-[5-(4,4,5,5-tetramethyl-1,3,2-dioxaborolan-2-yl)-pyridin-2-yl]urea (44). Ethylisocyanate (0.33 mL, 4.5 mmol) was added to a solution of 5-(4,4,5,5-tetramethyl-1,3,2-dioxaborolan-2-yl)pyridin-2-amine (1g, 4.5 mmol) in CHCl$_3$ (5 mL). The resulting mixture was heated in a microwave reactor at 110 °C for 1 h. Solvent was removed to give 1 g of the title product as a white solid. ^{1}H NMR (CDCl$_3$) δ 1.22 (t, 3H), 1.32 (s, 12H), 3.41 (m, 2H), 6.82 (d, 1H), 7.90 (dd, 1H), 8.52 (s, 1H), 8.62 (s, 1H), 9.40 (s, 1H). MS (ESI) m/z 292 [M + H]$^+$.

Methyl 2-(6-{[(Ethylamino)carbonyl]amino}pyridin-3-yl)-1,3-thia-zole-5-carboxylate (45e). N-Ethyl-N'-[5-(4,4,5,5-tetramethyl-1,3,2-dioxaborolan-2-yl)-pyridin-2-yl]urea (0.20 g, 0.69 mmol), methyl 2-bromo-1,3-thiazole-5-carboxylate (0.152 g, 0.69 mmol), tetrakistriphe-nylphosphine palladium (0.08 g, 0.069 mmol), and CsCO$_3$ (0.245 mg, 0.754 mmol) were taken together in a microwave vial and degassed with argon. Dioxane−water (4:1, 3 mL) was added, and the mixture was heated in a microwave reactor at 110 °C for 30 min. The reaction mixture was partitioned between water and EtOAc, and the layers were separated. The organic layer was washed with saturated aqueous NaHCO$_3$, water, and brine before being dried over MgSO$_4$. The solvent was removed, and the residue was purified by chromatography on silica gel (gradient eluting with 2% MeOH in CH$_2$Cl$_2$ to 3% MeOH in CH$_2$Cl$_2$ to give 0.123 g of material consistent with the title compound. ^{1}H NMR (DMSO-d_6) δ 1.09 (t, 3H), 3.16−3.22 (m, 2H), 3.86 (s, 3 H), 7.60 (d, 1H), 7.79 (t, 1H), 8.27 (dd, 1H), 8.49 (s, 1H), 8.83 (s, 1H), 9.56 (s, 1H). MS (ESI) m/z 307 [M + H]$^+$.

Compounds **15** and **45a−d** and **45f** were made similarly to the synthesis of ethyl 2-(6-{[(ethylamino)carbonyl]amino}pyridin-3-yl)-1,3-thiazole-5-carboxylate from compound **44** and the indicated aryl halide.

1-(3,3'-Bipyridine-6-yl)-3-ethylurea (15). Isolated as a solid (25 mg, 25%) from 84 mg of 3-iodopyridine. ^{1}H NMR (DMSO-d_6) δ 1.10 (t, 3H), 3.19−3.22 (m, 2H), 7.45−7.53 (m, 2H), 8.00 (brs, 1H), 8.07−8.10 (m, 2H), 8.57 (brs, 2H), 8.90 (s, 1H), 9.33 (s, 1H), 3.54 (brs, 1H). MS (ESI) m/z 243 [M + H]$^+$. HRMS [M + H]$^+$ 243.1246 (theoretical 243.1240).

Ethyl 2-(6-{[(Ethylamino)carbonyl]amino}pyridin-3-yl)-1,3-thia-zole-4-carboxylate (45a). Isolated as a solid (162 mg, 72%) from 165 mg ethyl 2-bromo-1,3-thiazole-4-carboxylate. ^{1}H NMR (DMSO-d_6) δ 1.09 (t, 3H), 1.31 (t, 3H), 3.14−3.22 (m, 2H), 4.32 (q, 2 H), 7.60 (d, 1H), 7.80 (brs, 1H), 8.21 (dd, 1H), 8.54 (s, 1H), 8.77 (s, 1H), 9.52 (s, 1H). MS (ESI) m/z 321 [M + H]$^+$.

Methyl 3-(6-{[(Ethylamino)carbonyl]amino}pyridin-3-yl)benzoate (45b). Isolated as a solid (110 mg, 54%) from 147 mg of methyl 3-bromobenzoate. ^{1}H NMR (DMSO-d_6) δ 1.09 (t, 3H), 3.15−3.24 (m, 2H), 3.88 (s, 3 H), 7.49 (d, 1H), 7.61 (t, 1H), 7.92−8.03 (m, 3H), 8.05 (dd, 1H), 8.16 (s, 1H), 8.53 (d, 1H) 9.32 (s, 1H). MS (ESI) m/z 300 [M + H]$^+$.

Methyl 4-(6-{[(Ethylamino)carbonyl]amino}pyridin-3-yl)benzoate (45c). Isolated as a solid (89 mg, 43%) from 148 mg of methyl 4-bromobenzoate. ^{1}H NMR (DMSO-d_6) δ 1.09 (t, 3H), 3.15−3.21 (m, 2H), 3.86 (s, 3 H), 7.50 (d, 1H), 7.83 (d, 2H), 7.96 (t, 1H), 8.01 (m, 2H), 8.09 (dd, 1H), 8.59 (d, 1H) 9.34 (s, 1H). MS (ESI) m/z 300 [M + H]$^+$.

Ethyl 6'-{[(Ethylamino)carbonyl]amino}-3,3'-bipyridine-5-car-boxylate (45d). Isolated as a solid (78 mg, 48%) from 118 mg of ethyl 5-bromonicotinate. ^{1}H NMR (DMSO-d_6) δ 1.09 (t, 3H), 1.35 (t, 3H), 3.14−3.25 (m, 2H), 4.37 (q, 2 H), 7.53 (d, 1H), 7.96 (t, 1H), 8.15 (dd, 1H), 8.47 (s, 1H), 8.64 (s, 1H), 9.04 (s, 1H), 9.13 (s, 1H), 9.37 (s, 1H). MS (ESI) m/z 315 [M + H]$^+$.

Ethyl 2-(6-{[(Ethylamino)carbonyl]amino}pyridin-3-yl)-1,3-ben-zothiazole-7-carboxylate (45f). Isolated as a solid (101 mg, 53%)

from 147 mg of ethyl 2-bromo-1,3-benzothiazole-7-carboxylate.[67] ^{1}H NMR (DMSO-d_6) δ 1.10 (t, 3H), 1.40 (t, 3H), 3.20 (m, 2H), 4.44 (q, 2 H), 7.68 (q, 2H), 7.82 (t, 1H), 8.10 (dd, 1H), 8.30 (d, 1H), 8.39 (dd, 1H), 8.94 (d, 1H), 9.59 (s, 1H). MS (ESI) m/z 371 [M + H]$^+$.

1-(4-Chloropyridin-2-yl)-3-ethylurea. A suspension of 4-chloropyridin-2-amine (2.186 g, 17 mmol), ethyl isocyanate (2.69 mL, 34.00 mmol), and chloroform (8 mL) was heated in the microwave at 100 °C for 1 h. The resultant solution was concentrated in vacuo to give the title compound in quantitative yield. No further purification was performed. ^{1}H NMR (DMSO-d_6) δ 9.31 (s, 1H), 8.16 (d, 1H), 7.63 (m, 1H), 7.59 (m, 1H), 7.03 (m, 1H), 3.16 (m, 2H), 1.07 (t, 3H). MS (ESI) m/z 200, 202 [M + H]$^+$.

1-(5-Bromo-4-chloropyridin-2-yl)-3-ethylurea (46a). A solution of 1-(4-chloropyridin-2-yl)-3-ethylurea (3.39 g, 16.98 mmol), N-bromosuccinimide (3.02 g, 16.98 mmol), acetonitrile (32 mL), and DMF (10 mL) were combined and heated at 80 °C for 2 h. Upon cooling to RT, a precipitate formed. Water was added, and the solid was collected and washed with water to give 2.78 g (59%) of the title compound which was used without further purification. ^{1}H NMR (DMSO-d_6) δ 9.37 (s, 1H), 8.44 (s, 1H), 7.92 (s, 1H), 7.17 (m, 1H), 3.15 (m, 2H), 1.06 (t, 3H). MS (ESI) m/z 278, 280 [M + H]$^+$.

4-Bromo-5-iodopyridin-2-amine. 4-Bromopyridin-2-amine (2.5g, 14.45 mmol) was dissolved in DMF (6 mL)/CHCl$_3$ (20 mL), 1-iodopyrrolidine-2,5-dione (6.50 g, 28.90 mmol) was added, and the mixture was stirred at 45 °C for 2 days. CHCl$_3$ was evaporated, and the remaining solution was poured into water (15 mL) and extracted with EtOAc (15 mL × 3). The organic phase was concentrated and purified by chromatography on silica gel, and elution with a hexanes−EtOAc gradient to give the title compound (3.2 g). ^{1}H NMR (DMSO-d_6) 4.51 (br, 2H), 6.80 (s, 1H), 8.35 (s, 1H). MS (ESI) m/z 299.9 [M + H]$^+$.

1-(4-Bromo-5-iodopyridin-2-yl)-3-ethylurea (46b). 4-Bromo-5-iodopyridin-2-amine (3.2g, 10.71 mmol) was dissolved in dry chloroform (15 mL). Ethylisocyanate (2.52 mL, 32.12 mmol) was added, and the reaction mixture was heated at reflux for 24 h. The reaction was cooled to room temperature, and hexanes were added. The resulting precipitate was collected by filtration to give the desired product (3.14 g). ^{1}H NMR (DMSO-d_6) 1.06 (t, 3H), 3.32 (q, 2H), 7.24 (br, 1H), 8.05 (s, 1H), 8.52 (s, 1H), 9.31 (s, 1H). MS (ESI) m/z 372 [M + H]$^+$.

Ethyl 4′-Chloro-6′-(3-ethylureido)-3,3′-bipyridine-5-carboxylate (47a). The 1-(5-bromo-4-chloropyridin-2-yl)-3-ethylurea **46a** (0.404 g, 1.45 mmol), ethyl 5-(4,4,5,5-tetramethyl-1,3,2-dioxaborolan-2-yl)-nicotinate (0.482 g, 1.74 mmol), and CsCO$_3$ (0.945 g, 2.90 mmol) were added to a microwave vessel. The vessel was degassed and purged with N$_2$. Tetrakis (triphenylphosphine)palladium(0) (0.168 g, 0.15 mmol) was added, and the vessel was degassed and purged with N$_2$. Dioxane (10 mL) and water (2.5 mL) were added, and the vessel was degassed and purged with N$_2$ three more times. The vessel was placed in the microwave and heated at 100 °C for 2 h. The organic layer was separated and concentrated in vacuo. After purification by silica gel chromatography (0−10% MeOH/CH$_2$Cl$_2$), the resultant solid was triturated with hot acetonitrile to give 0.339 g (67%) of the title compound. ^{1}H NMR (DMSO-d_6) δ 9.47 (s, 1H), 9.12 (m, 1H), 8.92 (m, 1H), 8.37 (m, 1H), 8.33 (s, 1H), 7.85 (s, 1H), 7.46 (m, 1H), 4.38 (q, 2H), 3.18 (m, 2H), 1.35 (t, 3H), 1.09 (t, 3H). MS (ESI) m/z 349, 351 [M + H]$^+$.

Ethyl 4′-Bromo-6′-(3-ethylureido)-3,3′-bipyridine-5-carboxylate (47b). 1-(4-Bromo-5-iodopyridin-2-yl)-3-ethylurea **45b** (1.33g, 3.59 mmol), ethyl 5-(4,4,5,5-tetramethyl-1, 3,2-dioxaborolan-2-yl) nicotinate (1.049 g, 3.59 mmol), tetrakis(triphenylphosphine)palladium(0) (0.415 g, 0.36 mmol), and K$_2$CO$_3$ (0.745 g, 5.39 mmol) were suspended in a mixture of DMF (10 mL) and water (1.0 mL). The suspension was degassed, purged with nitrogen, and heated at 100 °C for 1.5 h. The reaction mixture was cooled to room temperature and filtered; the filtrate was concentrated and purified by column chromatography on silica gel (0−10% MeOH/CH$_2$Cl$_2$) to give the title compound as a solid (1.32 g). ^{1}H NMR (CDCl$_3$) δ 1.29 (t, 3H), 1.45 (t, 3H), 3.45 (q, 2H), 4.47 (q, 2H), 7.30 (br, 1H), 8.12 (s, 1H), 8.38 (t, 1H), 8.84 (2s, 2 × H), 9.29 (s, 1H). MS (ESI) m/z 393, 395 [M + H]$^+$.

N-(4-Bromopyridin-2-yl)-N′-ethylurea (51). A mixture of 4-bromopyridin-2-amine (2 g, 11.6 mmol) and ethylisocyanate (0.91 mL, 11.6 mmol) in chloroform (10 mL) was heated at 110 °C for 2 h. The reaction mixture was concentrated under reduced pressure, and the residue was triturated with acetonitrile before being collected by filtration to give the title compound as a white solid (2.15 g). ^{1}H NMR (DMSO-d_6) δ 1.08 (t, 3H), 3.12−3.18 (m, 2H), 7.16 (dd, 1H), 7.65 (br s, 1H), 7.74 (s, 1H), 8.07 (d, 1H), 9.29 (s, 1H). MS (ESI) m/z 244, 246 [M + H]$^+$.

1-(4-Cyanopyridin-2-yl)-3-ethylurea. In a microwave reactor vessel fitted with a stir bar, 2-aminoisonicotinonitrile (2.0 g, 16.79 mmol) and ethylisocyanate (2.66 mL, 33.58 mmol) were suspended in CHCl$_3$ (8 mL). The vessel was sealed and heated at 100 °C for 1 h in a microwave reactor. The reaction mixture was concentrated under reduced pressure to provide 3.1 g of the title compound as a cream-colored solid. ^{1}H NMR (DMSO-d_6) δ 1.07 (t, 3H), 3.17 (m, 2H), 7.34 (m, 2H), 7.91 (s, 1H), 8.40 (d, 1H), 9.47 (s, 1H). LC MS (ESI) m/z 191, 193 [M + H].

N-Ethyl-N′-(4-phenylpyridin-2-yl)urea (52c). 1-(4-Bromopyridin-2-yl)-3-ethylurea **47** (500 mg, 2.05 mmol), phenylboronic acid (749 mg, 6.15 mmol), tetrakis(triphenylphosphine)palladium(0) (237 mg, 0.20 mmol), and CsCO$_3$ (2 g, 6.15 mmol) were suspended in a solution of dioxane−water (4:1). The reaction mixture was degassed and then heated to 110 °C in a microwave reactor for 30 min. The reaction mixture was filtered through a pad of Celite and then partitioned between EtOAc and water. The organic layer was dried over Na$_2$SO$_4$, filtered, and concentrated. The residue was purified by silica gel column chromatography (95:5 CH$_2$Cl$_2$/MeOH) to give 550 mg of the title compound as a white solid (95% yield). ^{1}H NMR (DMSO-d_6) δ 1.3 (t, 3H), 3.45 (m, 2H), 7.0 (s, 1H), 7.1 (d, 1H), 7.3−7.9 (m, 6H), 8.2 (d, 1H), 9.3 (br s, 1H). MS (ESI) m/z 242 [M + H]$^+$.

N-(3,4′-Bipyridin-2′-yl)-N′-ethylurea (52b). Prepared from 750 mg **47** and 630 mg of 3-pyridyl boronic acid as described for **48d** to afford 570 mg of the title compound. ^{1}H NMR (DMSO-d_6) δ 1.3 (t, 3H), 3.2 (m, 2H), 7.3 (d, 1H), 7.5 (m, 1H), 7.7 (s, 1H), 7.9−8.1 (m, 2H), 8.3 (d, 1H), 8.65 (d, 1H), 8.9 (s, 1H), 9.3 (s, 1H). MS (ESI) m/z 243 [M + H]$^+$.

1-(5-Bromo-4-cyanopyridin-2-yl)-3-ethylurea (47). A suspension of 1-(4-cyanopyridin-2-yl)-3-ethylurea (3.50 g, 18.40 mmol) and NBS (3.93 g, 22.08 mmol) in acetonitrile (100 mL) was heated at 60 °C. Upon heating, the suspension became homogeneous and turned dark-brown in color. After heating for 12 h, a precipitate formed. The mixture was cooled to room temperature, and the solids were filtered and washed first with water, and then with hexanes. Drying of the collected solids in vacuo gave 2.61 g of the title compound in a 52% yield. ^{1}H NMR (DMSO-d_6) δ 1.07 (t, 3H), 3.16 (m, 2H), 7.04 (m, 1H), 8.12 (s, 1H), 8.60 (s, 1H), 9.56 (s, 1H). MS (ESI) m/z 269, 271 [M + H]$^+$.

N-(5′-Bromo-3,4′-bipyridin-2′-yl)-N′-ethylurea (49c). Prepared from 165 mg of **52b** and 121 mg of NBS as described for **49** to afford 200 mg of the title compound. ^{1}H NMR (DMSO-d_6) δ 1.1 (t, 3H), 3.2 (m, 2H), 7.4 (m, 1H), 7.5−7.6 (m, 1H), 7.7 (s, 1H), 7.9 (d, 1H), 8.5 (d, 1H), 8.6 (s, 1H), 8.7 (d, 1H), 9.4 (s, 1H). MS (ESI) m/z 321, 323 [M + H]$^+$.

N-(5-Bromo-4-phenylpyridin-2-yl)-N′-ethylurea (53c). A mixture of 1-ethyl-3-(4-phenylpyridin-2-yl)urea **52c** (530 mg, 2.20 mmol) and N-bromosuccinamide (391 mg, 2.20 mmol) in DMF (5 mL) was heated at 80 °C for 2 h. Then the reaction mixture was partitioned between water and EtOAc. The layers were separated, and the organic layer was washed with 5% sodium thiosulfate solution, water, and brine before being dried (MgSO$_4$) and concentrated. The solid obtained was washed with acetonitrile and dried in vacuo to give off-white solid (250 mg). The acetonitrile wash was further concentrated and purified by normal phase chromatography (silica gel, 2−5% MeOH in CH$_2$Cl$_2$) to give additional 80 mg of the product as a white solid (330 mg total weight, 47%). ^{1}H NMR (CDCl$_3$) δ 1.21 (t, 3H), 3.33−3.42 (m, 2H), 6.9 (s, 1H), 7.25 (s, 1H), 7.42−7.46 (m, 5 H), 8.34 (s, 1H), 8.84 (s, 1H). MS (ESI) m/z 320, 322 [M + H]$^+$.

Ethyl 4′-Cyano-6′-(3-ethylureido)-3,3′-bipyridine-5-carboxylate (49). 1-(5-Bromo-4-cyanopyridin-2-yl)-3-ethylurea **47** (1.1 g, 4.09

mmol), ethyl 5-(4,4,5,5-tetramethyl-1,3,2-dioxaborolan-2-yl)nicotinate (1.35 g, 4.91 mmol), CsCO₃ (1.59 g, 4.91 mmol), and tetrakis-(triphenylphosphine)palladium(0) (422 mg, 0.41 mmol) were combined in a microwave vial and suspended in a solution of dioxane/water (4:1). The reaction mixture was degassed and then heated at 100 °C in a microwave reactor for 1 h. The reaction mixture was filtered through a pad of Celite, and the filtrate was partitioned between water and EtOAc. The layers were separated, and the aqueous was back extracted with EtOAc three times. The combined extract was washed with water and brine, dried over MgSO₄, and concentrated. The residue was purified by silica gel column chromatography (EtOAc/hexanes). The fractions containing product were concentrated, and the residue was triturated with acetonitrile. Isolation gave 970 mg of the title compound as a light-yellow solid (70% yield). ¹H NMR (DMSO-d₆) δ 1.1 (t, 3H), 1.35 (t, 3H), 3.2 (m, 2H), 4.4 (q, 2H), 7.25 (m, 1H), 8.1 (s, 1H), 8.5 (t, 1H), 8.6 (s, 1H), 9.05 (d, 1H), 9.2 (d, 1H), 9.6 (s, 1H). MS (ESI) m/z 340 [M + H]⁺.

Ethyl-6′-(3-ethylureido)-4′-(N′-hydroxycarbamimidoyl)-3,3′-bipyridine-5-carboxylate. Hydroxylamine (0.099 mL, 1.62 mmol) was added to a suspension of ethyl 4′-cyano-6′-(3-ethylureido)-3,3′-bipyridine-5-carboxylate **49** (500 mg, 1.47 mmol) in ethanol (10 mL), and the reaction mixture was heated at 65 °C for 3 h. After cooling, solvent was removed to give a white solid (457 mg). MS (ESI) m/z 373 [M + H]⁺.

Ethyl-6′-(3-ethylureido)-4′-(5-methyl-1,2,4-oxadiazol-3-yl)-3,3′-bipyridine-5-carboxylate. Acetic anhydride (0.057 mL, 0.60 mmol) was added to a solution of ethyl 6′-(3-ethylureido)-4′-(N′-hydroxycarbamimidoyl)-3,3′-bipyridine-5-carboxylate (150 mg, 0.40 mmol) in acetic acid (5 mL), and the reaction mixture was heated at 85 °C overnight The reaction mixture was diluted with water and extracted with EtOAc. The layers were separated, and the organic layer was dried over Na₂SO₄, filtered, and concentrated. The residue was purified by silica gel column chromatography (EtOAc—hexanes) to afford 110 mg of the title compound as a white solid. MS (ESI) m/z 397 [M + H]⁺.

Ethyl 5-[6-(Ethylcarbamoylamino)-4-(4-pyridyl)-3-pyridyl]-pyridine-3-carboxylate (54a). Dichlorobis(triphenylphosphine)-palladium(II) (60 mg, 0.086 mmol) as added to a solution of ethyl 4′-chloro-6′-(3-ethylureido)-3,3′-bipyridine-5-carboxylate (**46a**) (300 mg, 0.86 mmol) in dioxane (4 mL) in a 10 mL microwave vial. The mixture was stirred for 5—10 min before adding 4-pyridyl boronic acid (1.29 mmol, 1.5 equiv), followed by a solution of NaHCO₃ (0.774 g, 9.22 mmol) in water (2 mL). The vial was sealed and the mixture was stirred for 10 min and then heated in a microwave reactor at 120 °C for 4 h. EtOAc (3 mL) and brine (1 mL) were added to the reaction mixture, and the organic layer was separated and dried over Na₂SO₄. The volatiles were removed under vacuum, and the residue was purified by flash chromatography over silica gel, elution with isocratic 30% EtOAc in hexanes over 2 min, then gradient elution to 90% EtOAc in hexanes to give the title compound as a white solid in 65% yield. ¹H NMR (300 MHz, CD₃OD) δ 1.22 (t, 3H), 1.33 (t, 3H), 3.36 (q, 2H), 4.37 (q, 2H), 7.26 (d, 2H), 7.30 (s, 1H), 8.13 (s, 1H), 8.39 (s, 1H), 8.49 (d, 2H), 8.99 (s, 1H). MS (ESI) m/z 392 [M + H]⁺.

Ethyl 5-[6-(Ethylcarbamoylamino)-4-(3-pyridyl)-3-pyridyl]-pyridine-3-carboxylate (54b). Prepared from 530 mg of **53b** and 261 mg of ethyl 5-(4,4,5,5-tetramethyl-1,3,2-dioxaborolan-2-yl)-nicotinate as described for **49** to afford 160 mg of the title compound. ¹H NMR (DMSO-d₆) δ 1.09 (t, 3H), 1.27 (t, 3H), 3.14—3.24 (m, 2H), 4.28 (q, 2H), 7.35—7.39 (m, 1 H), 7.60 (s, 2H), 7.80 (s, 1H), 7.97 (s, 1H), 8.35 (s, 1H), 8.37 (s, 1H), 8.52 (d, 2H), 8.94 (s, 1H), 9.45 (s, 1H). MS (ESI) m/z 392 [M + H]⁺.

Ethyl 6′-(3-Ethylureido)-4′-phenyl-3,3′-bipyridine-5-carboxylate (54c). 1-(5-Bromo-4-phenylpyridin-2-yl)-3-ethylurea **53c** (230 mg, 0.72 mmol), ethyl 5-(4,4,5,5-tetramethyl-1,3,2-dioxaborolan-2-yl)-nicotinate (398 mg, 1.44 mmol), CsCO₃ (468 mg, 1.44 mmol), and tetrakis(triphenylphosphine)palladium(0) (83 mg, 0.07 mmol) in a sealed microwave reactor vial were degassed with N₂. Solvent (5 mL, dioxane–water, 4:1) was added, and the mixture was heated in a microwave reactor at 100 °C for 30 min. The reaction mixture was filtered through Celite, and the filtrate was partitioned between water

and EtOAc. The layers were separated, and the aqueous was back extracted with EtOAc three times. The combined extracts were washed with water and brine, dried over MgSO₄, and concentrated. The residue was purified by silica gel chromatography (1% to 3% MeOH in CH₂Cl₂) to obtain a off-white solid (155 mg, 55%) as the product. ¹H NMR (DMSO-d₆) δ 1.09 (t, 3H), 1.27 (t, 3H), 3.18—3.22 (m, 2H), 4.27 (q, 2H), 7.12—7.15 (m, 2H), 7.32—7.34 (m, 3H), 7.54 (s, 1H), 7.85 (brs, 1H), 7.95 (s, 1H), 8.33 (s, 1H), 8.50 (d, 1H), 8.9 (d, 1H), 9.4 (s, 1H). MS (ESI) m/z 391 [M + H]⁺.

5-Bromo-2-(3-ethylureido)isonicotinamide (55). A mixture of methyl 2-amino-5-bromoisonicotinate (3 g, 13 mmol) and ethyl-isocyanate (1.12 mL, 14.3 mmol) in chloroform (12 mL) was heated in a microwave reactor at 110 °C for 3 h. The reaction was concentrated, and 50 mL of 7N NH₃ in MeOH was added. The resulting mixture was stirred at room temperature overnight. After concentration of the solution, the residue was triturated with acetonitrile to give a white solid (3.5 g). ¹H NMR (DMSO-d₆) δ 1.06 (t, 3H), 3.1—3.3 (m, 2H), 7.1 (m, 1H), 7.6 (s, 1H), 8.0 (m, 1H), 8.3 (s, 1H), 9.3 (s, 1H). MS (ESI) m/z 287, 289 [M + H]⁺.

5-Bromo-2-(3-ethylureido)pyridine-4-carbothioamide (56). A mixture of 5-bromo-2-(3-ethylureido)isonicotinamide **55** (1.25 g, 4.35 mmol) and Lawesson's Reagent (1.76 g, 4.35 mmol) in THF (20 mL) was heated at 70 °C overnight. Solid precipitates were filtered and washed with THF. The filtrate was concentrated, and the residue was triturated with THF to isolate additional solids. The solids were combined to give 1 g of the title compound. ¹H NMR (DMSO-d₆) δ 1.07 (t, 3H), 3.1—3.3 (m, 2H), 7.37 (m, 1H), 7.5 (s, 1H), 8.3 (s, 1H), 9.3 (s, 1H), 9.8 (s, 1H), 10.3 (s, 1H). MS (ESI) m/z 303, 305 [M + H]⁺.

1-(5-Bromo-4-(4-tert-butylthiazol-2-yl)pyridin-2-yl)-3-ethylurea (57a). A mixture of 5-bromo-2-(3-ethylureido)pyridine-4-carbothioamide **56** (290 mg, 0.96 mmol) and 1-bromo-3,3-dimethylbutan-2-one (0.387 mL, 2.87 mmol) in acetonitrile (8 mL) was heated at 80 °C for 3 h. The reaction mixture was concentrated and purified by silica gel chromatography (1—3% MeOH in CH₂Cl₂) to give a white solid (230 mg, 63%). ¹H NMR (DMSO-d₆) δ 1.08 (t, 3H), 1.37 (s, 9H), 3.16—3.24 (m, 2H), 7.37 (brs, 1H), 7.64 (s, 1H), 8.35 (s, 1H), 8.50 (s, 1H), 9.36 (s, 1H). MS (ESI) m/z 383, 385 [M + H]⁺.

1-(5-Bromo-4-(4-hydroxy-4-(trifluoromethyl)-4,5-dihydrothiazol-2-yl)pyridin-2-yl)-3-ethylurea. A mixture of 5-bromo-2-(3-ethylureido)pyridine-4-carbothioamide **56** (1.1 g, 3.63 mmol) and 3-bromo-1,1,1-trifluoropropan-2-one (2.26 mL, 21.8 mmol) in acetonitrile (25 mL) was heated at 80 °C for 4 h. A clear solution resulted within an hour. The mixture was concentrated, and the residue was partitioned between water and EtOAc. The layers were separated, and the organic was washed with water and brine before being dried (MgSO₄) and concentrated to give a light-yellow solid. Purification by silica gel chromatography (2—5% MeOH in CH₂Cl₂) gave the title compound as a white solid (470 mg, 40%). ¹H NMR (DMSO-d₆) δ 1.06 (t, 3H), 3.12—3.18 (m, 2H), 3.60 (dd, 1H), 3.90 (dd, 1H), 7.13 (brs, 1H), 7.98 (s, 1H), 8.47 (s, 1H), 9.41 (s, 1H). MS (ESI) m/z 414, 416 [M + H]⁺.

N-{5-Bromo-4-[4-(trifluoromethyl)-1,3-thiazol-2-yl]pyridin-2-yl}-N′-ethylurea (57b). Trifluoroacetic anhydride (1.13 mL, 8.0 mmol) and triethylamine (1.113 mL, 8.0 mmol) were added sequentially to a mixture of 1-(5-bromo-4-(4-hydroxy-4-(trifluoromethyl)-4,5-dihydro-thiazol-2-yl)pyridin-2-yl)-3-ethylurea (2.2 g, 5.32 mmol) in acetonitrile (25 mL). The reaction mixture was allowed to stir overnight at room temperature. Because the reaction was not complete as determined by LC-MS, another 150 μL each of trifluoroacetic anhydride and triethylamine were added and stirring was continued for additional 3 h. The reaction mixture was concentrated, and the residue was partitioned between water and EtOAc. The layers were separated, and the organic layer was washed with aqueous NaHSO₄, water, and brine before being dried (MgSO₄) and concentrated. The residue was taken up in CH₂Cl₂ and some material precipitated. The solids were collected by filtration and dried (617 mg). The filtrate was concentrated, and the residue was purified by normal phase (silica gel, 1—3% MeOH in CH₂Cl₂) to give 520 mg of additional solid. Both solids were consistent with the title material for a total weight 1.14 g

(52%). ^{1}H NMR (DMSO-d_6) δ 1.07 (t, 3H), 3.11−3.17 (m, 2H), 7.24 (t, 1H), 8.35 (s, 1H), 8.50 (s, 1H), 8.77 (s, 1H), 9.34 (s, 1H). MS (ESI) m/z 420, 422 [M + H]$^+$.

Ethyl 4′-(4-tert-Butylthiazol-2-yl)-6′-(3-ethylureido)-3,3′-bipyridine-5-carboxylate (58a). A mixture of **57a** (220 mg, 0.57 mmol), ethyl 5-(4,4,5,5-tetramethyl-1,3,2-dioxaborolan-2-yl)nicotinate (318 mg, 1.15 mmol), CsCO$_3$ (374 mg, 1.15 mmol), and tetrakis-(triphenylphospine)palladium(0) (131 mg, 0.113 mmol) were taken in a microwave reactor vial and degassed with nitrogen. Dioxane (8 mL) and water (2 mL) were added, and the mixture was degassed again. The mixture has heated in a microwave reactor at 100 °C for 30 min. After cooling to room temperature, the mixture was filtered, and the filtrate was partitioned between water and EtOAc. The layers separated, and the organic layer was washed with aqueous NaHCO$_3$, water, and brine. The solution was dried (MgSO$_4$) and concentrated to afford a light-brown solid. The solid was triturated with acetonitrile to give a white solid (395 mg). ^{1}H NMR (DMSO-d_6) δ 1.05 (s, 9H), 1.09 (t, 3H), 1.30 (t, 3H), 3.16−3.24 (m, 2H), 4.33 (q, 2H), 7.41 (s, 1H), 7.66 (brs, 1H), 8.07 (d, 1H), 8.09 (s, 1H), 8.3 (s, 1H), 8.7 (d, 1H), 9.0 (s, 1H), 9.46 (s, 1H). MS (ESI) m/z 454 [M + H]$^+$.

Ethyl 6′-{[(Ethylamino)carbonyl]amino}-4′-[4-(trifluoromethyl)-1,3-thiazol-2-yl]-3,3′-bipyridine-5-carboxylate (58b). 1-(5-Bromo-4-(4-(trifluoromethyl)thiazol-2-yl)pyridin-2-yl)-3-ethylurea **57b** (2 g, 5.06 mmol), dicyclohexyl(2′,4′,6′-triisopropylbiphenyl-2-yl)phosphine (0.724 g, 1.52 mmol), Pd$_2$(dba)$_3$ (0.463 g, 0.51 mmol), ethyl 5-(4,4,5,5-tetramethyl-1,3,2-dioxaborolan-2-yl)nicotinate (2.80 g, 10.12 mmol), and CsCO$_3$ (3.63 g, 11.13 mmol) were placed in a round-bottom flask and degassed with nitrogen. Dioxane (30 mL) and water (5 mL) were added, and the mixture was degassed by bubbling though N$_2$ gas. The reaction mixture was heated at 95 °C for 1 h. After cooling to room temperature, the mixture was filtered through Celite and partitioned between water and EtOAc. The layers were separated, and the aqueous was back extracted twice with EtOAc. The combined extracts were washed with water and brine, dried (MgSO$_4$), and concentrated. The residue was purified by silica gel chromatography (hexanes/EtOAc) to give a light-brown solid that was triturated with acetonitrile to give a white solid (2.2 g) consistent with the title compound. ^{1}H NMR (DMSO-d_6) δ 1.11 (t, 3H), 1.31(t, 3H), 3.18−3.24 (m, 2H), 4.34 (q, 2H), 7.57 (brs, 1H), 8.16−8.18 (m, 1H), 8.21 (s, 1H), 8.39 (s, 1H), 8.58 (s, 1H), 8.75 (d, 1H), 9.10 (s, 1H), 9.52 (s, 1H). MS (ESI) m/z 466 [M + H]$^+$.

6-(3-Ethylureido)-4-(4-(trifluoromethyl)thiazol-2-yl)pyridin-3-yl-boronic Acid (59). A 2.0 M solution of i-PrMgCl in THF (800 mL, 1.60 mol, 2.53 equiv) was added to a suspension of **57b** (250 g, 0.633 mol) in anhydrous THF (6.25 L) −50 °C over 45−60 min (keeping the temperature below −35 °C). The reaction was stirred at −40 °C for an hour and then cooled to −78 °C. A 2.5 M solution of n-BuLi in hexane (1.42 L, 3.54 mol, 5.6 equiv) was added over 1 h (keeping the temperature below −65 °C). The reaction was stirred at −78 °C for 1 h before adding trimethylborate (775 mL, 10.7 equiv) in one portion. The mixture was allowed to warm to room temperature with stirring for 2 h. HCl (6N, 1.5 L) was added carefully, and the mixture was stirred for 45 min before being diluted with EtOAc (6.25 L) and water (3.5 L). The layers were separated, and the aqueous layer was adjusted to pH ~7−8 with sodium hydroxide before extraction with EtOAc (3 × 2 L). All organic layers were combined and concentrated under reduced pressure. The residue was suspended in water (3 L) and MTBE (1.5 L) with stirring for 1 h. Solid material was collected by vacuum filtration to give the first batch of material. The filtrate (water and MTBE) was concentrated under vacuum, and the residue was triturated with MTBE to give a second batch of material. The two batches were combined, triturated with water, and dried in a vacuum oven to give compound the title compound as an off-white solid (183 g, 79%). ^{1}H NMR (DMSO-d_6) δ 1.10 (t, 3H), 3.18 (m, 2H), 7.75 (brt, 1H), 7.91 (s, 1H), 8.18 (br, 2H), 8.31 (s, 1H), 8.64 (s, 1H), 9.31 (s, 1H). MS (ESI) m/z 361 [M + H]$^+$.

2-{6-{[(Ethylamino)carbonyl]amino}-4-[4-(trifluoromethyl)-1,3-thiazol-2-yl]pyridin-3-yl}-1,3-thiazole-5-carboxylate (33). A mixture of **59** (225 mg, 0.51 mmol), methyl 2-bromothiazole-5-carboxylate (113 mg, 0.51 mmol), CsCO$_3$ (166 mg, 0.51 mmol), and

tetrakis(triphenylphosphine)palladium(0) (59 mg, 0.05 mmol) were placed in a microwave reactor vial and degassed. Solvent (dioxane−water, 4:1, 10 mL) was added, and the reaction mixture was heated at 100 °C in a microwave reactor for 30 min. The reaction was filtered through Celite and partitioned between water and EtOAc. The layers were separated, and the aqueous was back extracted with EtOAc 3 times. The combined extracts were washed with water and brine, dried (MgSO$_4$), and concentrated. The residue was taken up in CH$_2$Cl$_2$ with 1% MeOH and solids precipitated. The solids were collected and dried in vacuo to afford 25 mg of material (MS (ESI) m/z 458 [M + H]$^+$) that was taken up in 5 mL MeOH. A 2N aqueous solution of LiOH (0.5 mL) was added, and the solution was stirred at 40 °C for 2 h. The solvent was removed, and the residue was dissolved in water. A 1N HCl aqueous solution was added, and solids that precipitated were collected and dried in vacuo. The material was consistent with title compound (15 mg, 8% over 2 steps). ^{1}H NMR (DMSO-d_6) δ 1.09 (t, 3H), 3.16−3.24 (m, 2H), 7.50 (s, 1H), 8.09 (s, 1H), 8.25 (s, 1H), 8.68 (d, 2H), 9.67 (s, 1H). MS (ESI) m/z 444 [M + H]$^+$. HRMS [M + H]$^+$ = 444.0412 (theoretical 444.0406).

2-(6-(3-Ethylureido)-4-(4-(trifluoromethyl)thiazol-2-yl)pyridin-3-yl)benzo[d]thiazole-7-carboxylate (55b). A mixture of **59** (300 mg, 0.68 mmol), ethyl 2-bromobenzo[d]thiazole-7-carboxylate (194 mg, 0.68 mmol), CsCO$_3$ (221 mg, 0.68 mmol), and tetrakis-(triphenylphosphine)palladium(0) (78 mg, 0.07 mmol) were placed in a microwave reactor vial and degassed. Solvent (dioxane−water, 4:1, 10 mL) was added, and the reaction mixture was heated in a microwave reactor at 100 °C for 30 min. The reaction was filtered through Celite and partitioned between water and EtOAc. The layers were separated, and the aqueous was back extracted with EtOAc 3 times. The combined extracts were washed with water and brine, dried (MgSO$_4$), and concentrated. The residue was purified by silica gel chromatography (1−3% gradient of MeOH in CH$_2$Cl$_2$) to afford 60 mg of a solid (MS (ESI) m/z 522 [M + H]$^+$) that was taken up in 2 mL of 1:1 THF−water. A 2N aqueous solution of LiOH (0.5 mL) was added, and the solution was stirred at 40 °C for 3 h. The solvent was removed, and the residue was dissolved in water. A 1N HCl aqueous solution was added, and solids that precipitated were collected and dried in vacuo. The material was consistent with title compound (40 mg, 12% over 2 steps). ^{1}H NMR (DMSO-d_6) δ 1.1 (t, 3H), 3.2 (m, 2H), 7.5 (s, 1H), 7.7 (t, 1H), 8.1 (d, 1H), 8.18 (s, 1H), 8.20 (d, 1H), 8.6 (s, 1H), 8.75 (s, 1H), 9.7 (s, 1H), 13.8 (s, 1H). MS (ESI) m/z 494 [M + H]$^+$. HRMS [M + H]$^+$ = 494.0558 (theoretical 494.0563).

2-(6-{[(Ethylamino)carbonyl]amino}pyridin-3-yl)-1,3-thiazole-5-carboxylic Acid (20). Methyl 2-(6-{[(ethylamino)carbonyl]amino}-pyridin-3-yl)-1,3-thiazole-5-carboxylate **44e** (0.185 g, 0.60 mmol) was taken in MeOH (6 mL), and 2N LiOH (1 mL) was added. The resulting mixture was stirred at 45 °C for 2 h. The solvent was removed, and the residue was dissolved in water before being acidified with 1N HCl. The precipitated solid was collected by filtration and washed with water and dried in vacuo to afford 0.17 g of material consistent with the title compound. ^{1}H NMR (DMSO-d_6) δ 1.09 (t, 3H), 3.16−3.22 (m, 2H), 7.60 (d, 1H), 7.81 (t, 1H), 8.26 (dd, 1H), 8.38 (s, 1H), 8.81 (s, 1H), 9.54 (s, 1H), 13.54 (brs, 1H). MS (ESI) m/z 293 [M + H]$^+$. HRMS [M + H]$^+$ 293.0716 (theoretical 293.0697).

Compounds **14**, **16−19**, **21**, **24−26**, and **25−34** were made similarly to the synthesis of **20**.

3-(6-(3-Ethylureido)pyridin-3-yloxy)benzoic Acid (14). Isolated as a solid (63 mg, 62%) from 100 mg of 3-(6-(3-ethylureido)pyridin-3-yloxy)benzoate. ^{1}H NMR (DMSO-d_6) δ 1.07 (t, 3H), 3.16−3.22 (m, 2H), 7.25−7.28 (m, 1H), 7.36 (s, 1H), 7.45−7.55 (m, 3H), 7.60−7.71 (m, 2H), 8.05 (s, 1H), 9.21 (s, 1H), 13.15 (s, 1H). ^{13}C NMR (DMSO-d_6, 126 MHz) δ 166.6, 157.9, 154.5, 150.3, 146.2, 138.8, 132.6, 130.9, 130.4, 123.8, 121.7, 116.8, 112.6, 33.8, 15.4. MS (ESI) m/z 302 [M + H]$^+$. HRMS [M + H]$^+$ 302.1139 (theoretical 302.1135).

2-(6-{[(Ethylamino)carbonyl]amino}pyridin-3-yl)-1,3-thiazole-4-carboxylic Acid (16). Isolated as a solid (53 mg, 65%) from 85 mg of **44a**. ^{1}H NMR (DMSO-d_6) δ 1.09 (t, 3H), 3.14−3.23 (m, 2H), 7.59 (d, 1H), 7.80 (t, 1H), 8.21 (dd, 1H), 8.46(s, 1H), 8.77 (s, 1H), 9.51 (s, 1H), 13.13 (brs, 1H). ^{13}C NMR (DMSO-d_6, 126 MHz) δ 164.7, 162.0, 154.8, 154.2, 147.9, 145.2, 136.0, 128.2, 122.1, 111.5, 33.9, 15.3.

MS (ESI) m/z 293 [M + H]$^+$. HRMS [M + H]$^+$ 293.0697 (theoretical 293.0703).

3-(6-{[(Ethylamino)carbonyl]amino}pyridin-3-yl)benzoic Acid (17). Isolated as a solid (43 mg, 56%) from 80 mg of **44b**. ^{1}H NMR (DMSO-d_6) δ 1.09 (t, 3H), 3.16–3.22 (m, 2H), 7.48–7.56 (m, 2H), 7.84–7.91 (m, 2H), 8.02–8.05 (m, 2H), 8.15 (s, 1H), 8.53 (s, 1H), 9.33 (s, 1H). ^{13}C NMR (101 MHz, DMSO-d_6) δ 167.8, 154.6, 153.0, 144.6, 136.9, 136.3, 135.0, 129.0, 128.8, 128.2, 128.1, 126.6, 111.5, 33.8, 15.3. MS (ESI) m/z 286 [M + H]$^+$. HRMS [M + H]$^+$ 286.1184 (theoretical 286.1186).

4-(6-{[(Ethylamino)carbonyl]amino}pyridin-3-yl)benzoic Acid (18). Isolated as a solid (56 mg, 92%) from 64 mg of **44c**. ^{1}H NMR (DMSO-d_6) δ 1.09 (t, 3H), 3.15–3.21 (m, 2H), 3.86 (s, 3 H), 7.50 (d, 1H), 7.80 (d, 2H), 7.98 (t, 1H), 7.99 (d 2H), 8.07 (dd, 1H), 8.59 (d, 1H), 9.33 (s, 1H), 12.98 (brs, 1H). ^{13}C NMR (DMSO-d_6, 126 MHz) δ 167.1, 154.4, 153.3, 144.7, 141.2, 136.5, 130.0, 129.4, 127.4, 126.0, 111.5, 33.9, 15.4. MS (ESI) m/z 286 [M + H]$^+$. HRMS [M + H]$^+$ = 286.1189 (theoretical 286.1186).

6'-{[(Ethylamino)carbonyl]amino}-3,3'-bipyridine-5-carboxylic Acid (19). Isolated as a solid (14 mg, 25%) from 63 mg of **44d**. ^{1}H NMR (DMSO-d_6) δ 1.09 (t, 3H), 3.15–3.23 (m, 2H), 7.53 (d, 1H), 7.95 (t, 1H), 8.14 (dd, 1H), 8.45 (t, 1H), 8.63 (s, 1H), 9.02 (s, 1H), 9.11 (s, 1H), 9.35 (s, 1H), 13.51 (brs, 1H). ^{13}C NMR (DMSO-d_6, 126 MHz) δ 167.5, 166.6, 155.2, 154.4, 154.2, 152.6, 146.0, 136.9, 134.4, 127.1, 126.9, 126.7, 125.0, 122.1, 111.7, 33.9, 15.2. MS (ESI) m/z 287 [M + H]$^+$. HRMS [M + H]$^+$ = 287.1134 (theoretical 287.1139).

2-(6-{[(Ethylamino)carbonyl]amino}pyridin-3-yl)-1,3-benzothiazole-7-carboxylic Acid (21). Isolated as a solid (38 mg, 92%) from 45 mg of **44f**. ^{1}H NMR (DMSO-d_6) δ 1.09 (t, 3H), 3.18–3.23 (m, 2H), 7.48 (t, 1H), 7.58 (d, 1H), 7.87–7.91 (m, 2H), 7.80 (d, 1H), 8.31 (dd, 1H), 8.86 (d, 1H), 9.52 (s, 1H). MS (ESI) m/z 343 [M + H]$^+$. HRMS [M + H]$^+$ = 343.0843 (theoretical 343.0859).

4'-Chloro-6'-(3-ethylureido)-3,3'-bipyridine-5-carboxylic Acid (24). Isolated as a solid (126 mg, 91%) from 151 mg of **46a**. ^{1}H NMR (DMSO-d_6) δ 1.09 (t, 3H), 3.18 (q, 2H), 7.51 (s, 1H), 7.85 (s, 1H), 8.33 (s, 2H), 8.88 (s, 1H), 9.10 (s, 1H), 9.45 (s, 1H), 13.71 (s, 1H). ^{13}C NMR (DMSO-d_6, 126 MHz) δ 166.0, 154.1, 153.2, 149.4, 148.9, 142.4, 137.5, 131.0, 126.2, 124.5, 111.2, 33.9, 15.2. MS (ESI) m/z 321, 323 [M + H]$^+$. HRMS [M + H]$^+$ = 321.0758 (theoretical 321.0748).

4'-Bromo-6'-(3-ethylureido)-3,3'-bipyridine-5-carboxylic Acid (25). Isolated as a solid (3.6 g, 68%) from 5.39 g of **46b**. ^{1}H NMR (DMSO-d_6) δ 1.09 (t, 3H), 3.18 (q, 2H), 7.48 (s, 1H), 8.03 (s, 1H), 8.28 (s, 1H), 8.32 (s, 1H), 8.86 (s, 1H), 9.11 (s, 1H), 9.44 (s, 1H), 13.60 (s, 1H). MS (ESI) m/z 365, 367 [M + H]$^+$. HRMS [M + H]$^+$ = 365.0248 (theoretical 365.0243).

6'-(3-Ethylureido)-4'-(5-methyl-1,2,4-oxadiazol-3-yl)-3,3'-bipyridine-5-carboxylic Acid (26). Isolated as a solid (75 mg, 73%) from ethyl 6'-(3-ethylureido)-4'-(5-methyl-1,2,4-oxadiazol-3-yl)-3,3'-bipyridine-5-carboxylate **50** (110 mg, 0.28 mmol). ^{1}H NMR (DMSO-d_6) δ 1.11 (t, 3H), 2.58 (s, 3H), 3.20 (m, 2H), 7.55 (t, 1H), 8.13 (s, 1H), 8.21 (s, 1H), 8.36 (s, 1H), 8.68 (s, 1H), 9.05 (s, 1H), 9.51 (s, 1H), 13.46 (brs, 1H). MS (ESI) m/z 369 [M + H]$^+$. HRMS [M + H]$^+$ = 369.1324 (theoretical 369.1305).

6'-{[(Ethylamino)carbonyl]amino}-3,3':4',3''-terpyridine-5-carboxylic Acid (28). Isolated as a solid (57 mg, 45%) from 135 mg (0.34 mmol) **54b**. ^{1}H NMR (DMSO-d_6) δ 1.09 (t, 3H), 3.14–3.24 (m, 2H), 7.35–7.39 (m, 1 H), 7.57 (d, 1H), 7.66 (s, 1H), 7.94–7.95 (m, 2H), 8.31–8.33 (m, 3H), 8.51 (d, 1H), 8.88 (d, 1H), 9.54 (s, 1H). ^{13}C NMR (DMSO-d_6, 126 MHz) δ 166.2, 154.5, 153.7, 152.6, 149.2, 149.1, 148.6, 148.2, 146.3, 137.4, 136.6, 134.0, 132.4, 128.0, 124.9, 123.4, 111.9, 33.9, 15.3. MS (ESI) m/z 364 [M + H]$^+$. HRMS [M + H]$^+$ = 364.1421 (theoretical 364.1404).

6'-{[(Ethylamino)carbonyl]amino}-4'-phenyl-3,3'-bipyridine-5-carboxylic Acid (29). Isolated as a solid (124 mg, 90%) from 140 mg of **50c**. ^{1}H NMR (DMSO-d_6) δ 1.09 (t, 3H), 3.14–3.22 (m, 2H), 7.11–7.15 (m, 2H), 7.32–7.34 (m, 3H), 7.53 (s, 1H), 7.90 (brs, 1H), 7.92 (s, 1H), 8.30 (s, 1H), 8.44 (d, 1H), 8.87 (s, 1H), 9.40 (s, 1H). ^{13}C NMR (DMSO-d_6, 126 MHz) δ 165.9, 154.5, 153.6, 153.3, 149.7, 148.3, 147.9, 138.0, 137.3, 133.1, 129.0, 128.6, 128.2, 126.0, 124.5,

111.9, 33.9, 15.3; .MS (ESI) m/z 363 [M + H]$^+$. HRMS [M + H]$^+$ = 363.1468 (theoretical 363.1452).

4'-(4-tert-Butylthiazol-2-yl)-6'-(3-ethylureido)-3,3'-bipyridine-5-carboxylic Acid (30). Isolated as a solid (78 mg, 83%) from 100 mg of **58a**. ^{1}H NMR (DMSO-d_6) δ 1.05 (s, 9H), 1.10 (t, 3H), 3.16- 3.27 (m, 2H), 7.39 (s, 1H), 7.66 (br s, 1H), 8.03 (s, 1H), 8.06 (s, 1H), 8.28 (s, 1H), 8.65 (d, 1H), 9.00 (s, 1H), 9.44 (s, 1H), 13.43 (s, 1H). MS (ESI) m/z 426 [M + H]$^+$. HRMS [M + H]$^+$ = 426.1596 (theoretical 426.1594).

6'-{[(Ethylamino)carbonyl]amino}-4'-[4-(trifluoromethyl)-1,3-thiazol-2-yl]-3,3'-bipyridine-5-carboxylic Acid (31). Isolated as a solid (60 mg, 88%) from 70 mg of **58b**. ^{1}H NMR (DMSO-d_6) δ 1.11 (t, 3H), 3.18–3.24 (m, 2H), 7.57 (brs, 1H), 8.15–8.18 (m, 1H), 8.22 (s, 1H), 8.37 (s, 1H), 8.57 (s, 1H), 8.72 (s, 1H), 9.08 (s, 1H), 9.51 (s, 1H), 13.53 (s, 1H). LC MS (ESI) m/z 438.0848 [M + H]$^+$; HRMS [M + H]$^+$ = (theoretical 438.0842).

6'-(3-Ethylureido)-4-(4-pyridyl)-3,3'-bipyridine-5-carboxylic Acid (27). A 1N solution of LiOH (0.3 mL) was added dropwise to a solution of **54a** (50 mg, 0.13 mmol) in methanol. The reaction progress was followed by LC/MS, and the reaction was stopped upon reaching above 90–95% conversion to product. The methanol was removed partially under reduced pressure, and EtOAc (5 mL) was added. The mixture was cooled to 4 °C, acidified to pH ~2 with 10% solution of HCl, and extracted with EtOAc. The organic layer was separated and dried with Na$_2$SO$_4$. Volatiles were removed under reduced pressure to give a solid residue, which was dried to give the desired product. ^{1}H NMR (CD$_3$OD) δ 1.22 (t, 3H), 3.36 (q, 2H), 7.68 (s, 1H), 8.05 (brs, 2H), 8.53 (brs, 2H), 8.88 (brs, 3H), 9.22 (brs, 1H). ^{13}C NMR (DMSO-d_6, 126 MHz) δ 165.6, 153.8, 153.7, 154.4, 152.7, 148.6, 148.3, 145.2, 143.2, 138.4, 132.0, 126.5, 126.9, 123.8, 111.5, 33.9, 15.3. MS (ESI) m/z 369 [M + H]$^+$. HRMS [M + H]$^+$ = 364.1407 (theoretical 364.1404).

2-(6-{[(Ethylamino)carbonyl]amino}pyridin-3-yl)-1,3-thiazole-5-carboxamide (22). HATU (0.078 mg, 0.225 mmol) was added to a solution of 2-(6-{[(ethylamino)carbonyl]amino}pyridin-3-yl)-1,3-thiazole-4-carboxylic acid **20** (60 mg, 0.205 mmol), Et$_3$N (84 μL, 0.41 mmol)), and cumylamine (28 mg, 0.205 mmol) in 3 mL of DMF. After stirring at room temperature for 2 h, the mixture was diluted with water and extracted with EtOAc. Solids, which precipitated during the workup, were collected by filtration, rinsed with water and EtOAc, and dried in vacuo to afford 20 mg of a solid (MS (ESI) m/z 410 [M + H]$^+$) that was dissolved 1 mL of TFA (1 mL) with stirring at room temperature overnight. The TFA was removed under reduced pressure, and the residue was taken up in aqueous NaHCO$_3$. Solids that precipitated were collected by filtration, washed with water, and dried in vacuo to afford 15 mg (25% over 2 steps) of material consistent with the title compound. ^{1}H NMR (DMSO-d_6) δ 1.1 (t, 3H), 3.2 (m, 2H), 7.6 (m, 2H), 8.15 (m, 1H), 8.3 (brs, 1H), 8.2 (d, 1H), 8.4 (s, 1H), 8.77 (d, 1H), 9.5 (s, 1H). MS (ESI) m/z 292 [M + H]$^+$. HRMS [M + H]$^+$ = 292.0875 (theoretical 292.0862).

2-(6-{[(Ethylamino)carbonyl]amino}pyridin-3-yl)-1,3-benzothiazole-7-carboxamide (23). Following the procedure for the synthesis of compound **22**, the title compound was isolated as a solid (43 mg, 61%) from 70 mg of compound **21**. ^{1}H NMR (DMSO-d_6) δ 1.10 (t, 3H), 3.16–3.23 (m, 2H), 7.60–7.66 (m, 2H), 7.82 (brs, 2H), 8.08 (d, 1H), 8.17 (d, 1H), 8.38 (dd, 1H), 8.41(s, 1H), 8.92 (d, 1H), 9.56 (s, 1H). MS (ESI) m/z 342 [M + H]$^+$. HRMS [M + H]$^+$ = 342.1010 (theoretical 342.1019).

6'-(3-Ethylureido)-4'-(4-(trifluoromethyl)thiazol-2-yl)-3,3'-bipyridine-5-carboxamide (32). Following the procedure for the synthesis of compound **22**, the title compound was isolated as a solid (9 mg, 14%) from 65 mg of compound **31**. Isolated as a solid (9 mg, 54%). ^{1}H NMR (DMSO-d_6) δ 1.09 (t, 3H), 3.18–3.24 (m, 2H), 7.45 (brs, 1H), 7.65 (s, 1H), 8.16 (s, 1H), 8.18 (s, 1H), 8.24 (s, 1H), 8.35 (s, 1H), 8.55 (d, 1H), 8.60 (d, 1H), 9.05 (s, 1H), 9.49 (s, 1H). ^{13}C NMR (DMSO-d_6, 126 MHz) δ 166.5, 166.1, 165.6, 155.0, 154.1, 153.7, 149.5, 142.8, 140.0, 135.7, 127.4, 127.3, 126.8, 126.7, 125.3, 120.7, 120.3, 111.1, 34.0, 15.2. MS (ESI) m/z 437 [M + H]$^+$. HRMS [M + H]$^+$ = 437.0994 (theoretical 437.1002).

1-Ethyl-3-(5′-(hydrazinecarbonyl)-4-(4-(trifluoromethyl)thiazol-2-yl)-3,3′-bipyridin-6-yl)urea. A solution of 150 mg (0.32 mmol) of 1-ethyl-3-(5′-(hydrazinecarbonyl)-4-(4-(trifluoromethyl)thiazol-2-yl)-3,3′-bipyridin-6-yl)urea **58b** and 0.30 mL (0.97 mmol) of hydrazine in 20 mL ethanol was heated at reflux for 5 h. Solvent was removed, and the solid residue was triturated with 10% MeOH in CH_2Cl_2. The solids were collected and dried in vacuo to afford 101 mg (69%) of the title compound. ^1H NMR (DMSO-d_6) δ 1.09 (t, 3H), 3.1−3.3 (m, 2H), 4.6 (brs, 2H), 7.55 (m, 1H), 8.13 (s, 1H), 8.23 (s, 1H), 8.34 (s, 1H), 8.55 (s, 1H), 8.59 (s, 1H), 8.99 (s, 1H), 9.48 (s, 1H), 9.97 (s, 1H). MS (ESI) m/z 452 [M + H]$^+$.

1-Ethyl-3-(5′-(5-oxo-4,5-dihydro-1,3,4-oxadiazol-2-yl)-4-(4-(trifluoromethyl)thiazol-2-yl)-3,3′-bipyridin-6-yl)urea (35). Carbonyldiimidazole (56.6 mg, 0.35 mmol) was added to a solution of 1-ethyl-3-(5′-(hydrazinecarbonyl)-4-(4-(trifluoromethyl)thiazol-2-yl)-3,3′-bipyridin-6-yl)urea (105 mg, 0.23 mmol) and diisopropylethylamine (0.061 mL, 0.35 mmol) in DMF (1.5 mL), and the mixture was stirred at room temperature for 1.5 h. The reaction mixture was diluted with water and extracted with 5% methanol in CH_2Cl_2. The combined extract was washed with water and brine and dried over $MgSO_4$ and concentrated. The residue was purified by silica gel chromatography (2−8% MeOH gradient in CH_2Cl_2) to give the title compound as a white solid (65 mg). ^1H NMR (DMSO-d_6) δ 1.10 (t, 3H), 3.16−3.28 (m, 2H), 7.55 (brs, 1H), 8.09 (s, 1H), 8.22 (s, 1H), 8.37 (s, 1H), 8.57 (s, 1H), 8.62 (s, 1H), 8.97 (s, 1H), 9.50 (s, 1H), 12.80 (s, 1H). ^{13}C NMR (DMSO-d_6, 126 MHz) δ 166.2, 154.3, 154.2, 154.1, 152.4, 151.8, 149.3, 145.3, 142.8, 139.3, 134.0, 132.7, 126.3, 123.6, 120.1, 120.3, 110.3, 33.9, 15.3. MS (ESI) m/z 437 [M + H]$^+$. HRMS [M + H]$^+$ = 478.0918 (theoretical 478.0903).

1-(5′-(2-Acetylhydrazinecarbonyl)-4-(4-(trifluoromethyl)thiazol-2-yl)-3,3′-bipyridin-6-yl)-3-ethylurea. HATU (89 mg, 0.23 mmol) was added to a solution of 85 mg (0.19 mmol) of 6′-{[(ethylamino)carbonyl]amino}-4′-[4-(trifluoromethyl)-1,3-thiazol-2-yl]-3,3′-bipyridine-5-carboxylic acid **31**, triethylamine (54 μL, 0.39 mmol), and acetohydrazide (14.1 mg, 0.19 mmol) in 2 mL of DMF, and the mixture was stirred at room temperature for 1 h. The mixture was diluted with EtOAc and washed 3 times with water and once with brine. Drying ($MgSO_4$) and removal of solvent gave an oil (158 mg) that was purified by reverse phase HPLC (acetonitrile−water gradient with 0.1% TFA) to afford 48 mg (52%) of the title compound as a solid. ^1H NMR (DMSO-d_6) δ 1.10 (t, 3H), 2.58 (s, 3H), 3.1−3.3 (m, 2H), 4.6 (brs, 2H), 7.54 (brs, 2H), 7.5−7.6 (m, 1H), 8.23 (s, 1H), 8.29 (s, 1H), 8.4 (s, 1H), 8.56 (s, 1H), 8.69 (s, 1H), 9.15 (s, 1H), 9.51 (s, 1H). MS (ESI) m/z 494 [M + H]$^+$.

1-Ethyl-3-(5′-(5-methyl-1,3,4-oxadiazol-2-yl)-4-(4-(trifluoromethyl)thiazol-2-yl)-3,3′-bipyridin-6-yl)urea (36). Triphenylphosphine (306 mg, 2.33 mmol), CCl_4 (0.114 mL, 1.17 mmol), and triethylamine (0.316 mL, 2.33 mmol) were added to a mixture of 1-(5′-(2-acetylhydrazinecarbonyl)-4-(4-(trifluoromethyl)thiazol-2-yl)-3,3′-bipyridin-6-yl)-3-ethylurea (184 mg, 0.389 mmol) in CH_2Cl_2 (5 mL). The resulting mixture was allowed to stir overnight at room temperature. The mixture was partitioned between water and CH_2Cl_2. The layers were separated, and the aqueous layer was back extracted 3 times with CH_2Cl_2. The combined extracts were washed with water, dried ($MgSO_4$), and concentrated, and the residue was purified by normal phase chromatography (1−3% gradient of MeOH in CH_2Cl_2) to give the title compound as a white solid (48 mg, 26%). ^1H NMR (DMSO-d_6) δ 1.10 (t, 3H), 2.58 (s, 3H), 3.18−3.22 (m, 2H), 7.54 (brs, 1H) 8.23 (s, 1H), 8.28 (s, 1H), 8.40 (s, 1H), 8.56 (s, 1H), 8.69 (s, 1H), 9.15 (d, 1H), 9.51 (s, 1H). MS (ESI) m/z 476 [M + H]$^+$. HRMS [M + H]$^+$ = 476.1117 (theoretical 476.1111).

N-(1-(Dimethylamino)ethylidene)-6′-(3-ethylureido)-4′-(4-(trifluoromethyl)thiazol-2-yl)-3,3′-bipyridine-5-carboxamide. A mixture of 6′-(3-ethylureido)-4′-(4-(trifluoromethyl)thiazol-2-yl)-3,3′-bipyridine-5-carboxamide **32** (270 mg, 0.62 mmol) in 1,1-dimethoxy-N,N-dimethylethanamine (10 mL, 68.40 mmol) was heated to 120 °C for 1 h. After cooling to room temperature, solids that precipitated were filtered, rinsed acetonitrile, and dried in vacuo. The solids were consistent with the title compound, 178 mg (57%). ^1H NMR (DMSO-d_6) δ 1.11 (t, 3H), 2.29 (s, 3H), 3.11 (s, 3H), 3.14 (s, 3H), 3.18−3.22

(m, 2H), 7.6 (m, 1H) 8.14 (s, 1H), 8.2 (s, 1H), 8.37 (s, 1H), 8.55 (s, 1H), 8.63 (s, 1H), 9.16 (d, 1H), 9.48 (s, 1H). MS (ESI) m/z 506 [M + H]$^+$.

1-Ethyl-3-(5′-(3-methyl-1,2,4-oxadiazol-5-yl)-4-(4-(trifluoromethyl)thiazol-2-yl)-3,3′-bipyridin-6-yl)urea (37). A mixture of N-(1-(dimethylamino)ethylidene)-6′-(3-ethylureido)-4′-(4-(trifluoromethyl)thiazol-2-yl)-3,3′-bipyridine-5-carboxamide (80 mg, 0.16 mmol), hydroxylamine hydrochloride (13.20 mg, 0.19 mmol), 2N NaOH (0.038 mL, 0.19 mmol), and 70% aqueous acetic acid (2 mL) in 3 mL of dioxane was heated at 80 °C for 30 min. After cooling to room temperature, solvent was removed and the residue was partitioned between water and CH_2Cl_2. The layers separated, and the aqueous was back extracted 3 times with CH_2Cl_2. Solids precipitated from the CH_2Cl_2 solution. The solids were filtered and dried in vacuo to give the title compound as a white solid (55 mg, 73%). ^1H NMR (DMSO-d_6) δ 1.10 (t, 3H), 2.31 (s, 3H), 3.05−3.28 (m, 2H), 7.74 (brs, 1H), 8.24 (s, 1H), 8.40 (s, 2H), 8.56 (s, 1H), 8.77 (d, 1H), 9.25 (d, 1H), 9.60 (s, 1H). ^{13}C NMR (DMSO-d_6, 126 MHz) δ 166.3, 166.2, 158.2, 154.3, 153.9, 149.1, 148.8, 148.7, 142.8, 139.6, 137.7, 132.4, 126.4, 125.7, 124.6, 120.3, 112.6, 110.3, 33.9, 15.3, 11.2, 10.1. MS (ESI) m/z 476 [M + H]$^+$. HRMS [M + H]$^+$ = 476.1107 (theoretical 476.1111).

1-(5′-(3,5-Dimethylisoxazol-4-yl)-4-(4-(trifluoromethyl)thiazol-2-yl)-3,3′-bipyridin-6-yl)-3-ethylurea (38). 3-Bromo-5-(4,4,5,5-tetramethyl-1,3,2-dioxaborolan-2-yl)pyridine (596 mg, 2.10 mmol), 1-(5-bromo-4-(4-(trifluoromethyl)thiazol-2-yl)pyridin-2-yl)-3-ethylurea (**53b**) (830 mg, 2.10 mmol), tris(dibenzylideneacetone)dipalladium(0) (192 mg, 0.21 mmol), 2-dicyclohexylphosphino-2′,4′,6′-tri-*iso*-propyl-1,1′-biphenyl (300 mg, 0.63 mmol), and Na_2CO_3 (223 mg, 2.10 mmol) were taken in a round bottomed flask, and the flask was flushed with nitrogen. Solvent (5:1; acetonitrile−water, 10 mL) was added and degassed with nitrogen, and the mixture was heated at 100 °C for 3 h. The reaction mixture was filtered, and the filtrate was concentrated under reduced pressure. The resulting crude residue was partitioned between water and EtOAc. The layers were separated, and the aqueous was back extracted with EtOAc three times. The combined organic layers were washed with water and brine, dried over $MgSO_4$, and concentrated under reduced pressure. The residue obtained was purified by normal phase chromatography (gradient of MeOH in CH_2Cl_2) to give a white solid (483 mg) consistent with 1-(5′-bromo-4-(4-(trifluoromethyl)-thiazol-2-yl)-3,3′-bipyridin-6-yl)-3-ethylurea **57b** (MS (ESI) m/z 472, 474 [M + H]$^+$). The solid (100 mg, 0.21 mmol), 3,5-dimethyl-4-(4,4,5,5-tetramethyl-1,3,2-dioxaborolan-2-yl)isoxazole (70.9 mg, 0.32 mmol), dicyclohexyl(2′,4′,6′-triisopropylbiphenyl-2-yl)phosphine (30.3 mg, 0.06 mmol), tris(dibenzylideneacetone)dipalladium(0) (19.39 mg, 0.02 mmol), and Na_2CO_3 (33.7 mg, 0.32 mmol) were placed in a microwave reaction vial and degassed with nitrogen. Acetonitrile (4 mL) and water (0.8 mL) were added, and the mixture was heated in a microwave reactor at 100 °C for 40 min. After cooling to room temperature, the mixture was partitioned between water and EtOAc. The layers were separated, and the aqueous layer was back extracted 3 times with EtOAc. Combined extracts were washed with water and brine. Drying ($MgSO_4$) and removal of solvent was followed by silica gel chromatography (1−3% gradient MeOH in CH_2Cl_2) of the residue to give a white solid (63 mg) with some impurities. Further purification with a second silica gel chromatography (1−3% gradient MeOH in CH_2Cl_2) afforded a white solid (40 mg) consistent with the title compound. ^1H NMR (DMSO-d_6) δ 1.10 (t, 3H), 2.15 (s, 3H), 2.36 (s, 3H), 3.08−3.29 (m, 2H), 7.58 (br s, 1H), 7.80 (s, 1H), 8.21 (s, 1H), 8.37 (s, 1H), 8.55 (d, 1H), 8.57 (s, 1H), 8.67 (d, 1H), 9.48 (s, 1H). MS (ESI) m/z 489 [M + H]$^+$. HRMS [M + H]$^+$ = 489.1334 (theoretical 489.1315).

1-(5′-Cyano-4-(4-(trifluoromethyl)thiazol-2-yl)-3,3′-bipyridin-6-yl)-3-ethylurea (39). 1-(5-Bromo-4-(4-(trifluoromethyl)thiazol-2-yl)-pyridin-2-yl)-3-ethylurea **53b** (300 mg, 0.76 mmol), $CsCO_3$ (495 mg, 1.52 mmol), tetrakis(triphenylphosphine)palladium (0) (88 mg, 0.08 mmol), and 5-(4,4,5,5-tetramethyl-1,3,2-dioxaborolan-2-yl)-nicotinonitrile (349 mg, 1.52 mmol) were placed in a microwave reaction vial and degassed with nitrogen. Then dioxane−water (4:1, 6

mL) was added, and the mixture has heated in a microwave reactor at 100 °C for 30 min. The reaction mixture was partitioned between water and EtOAc, and layers were separated. The aqueous layer was back extracted with EtOAc (3 times). The combined EtOAc layers were washed with aqueous NaHCO₃, water, and brine before being dried (MgSO₄). The solvent was removed, and the residue was triturated with acetonitrile to give the title compound as a white solid (270 mg, 85%). ^{1}H NMR (DMSO-d_6) δ 1.09 (t, 3H), 3.16–3.22 (m, 2H), 7.49 (t, 1 H), 8.22 (s, 1H), 8.36 (s, 1H), 8.38 (d, 1H), 8.60 (s, 1H), 8.76 (s, 1H), 9.04 (s, 1H), 9.52 (s, 1H). MS (ESI) m/z 419 [M + H]$^+$. HRMS [M + H]$^+$ = 419.0893 (theoretical 419.0896).

1-(5′-(2H-Tetrazol-5-yl)-4-(4-(trifluoromethyl)thiazol-2-yl)-3,3′-bipyridin-6-yl)-3-ethylurea (40). A mixture of 1-(5′-cyano-4-(4-(trifluoromethyl)thiazol-2-yl)-3,3′-bipyridin-6-yl)-3-ethylurea (60 mg, 0.14 mmol), NaN₃ (18.65 mg, 0.29 mmol), and NH₄Cl (14.57 mg, 0.27 mmol) in DMF (1.5 mL) was heated at 100 °C for 6 h. Solvent was removed, and the residue was purified by reverse phase HPLC (acetonitrile–water gradient with 0.1% TFA) to afford the title compound as a white solid (23 mg, 36% yield). ^{1}H NMR (DMSO-d_6) δ 1.09 (t, 3H), 3.17–3.22 (m, 2H), 7.53 (t, 1 H), 8.25 (s, 1H), 8.35 (s, 1H), 8.40 (s, 1H), 8.55 (s, 1H), 8.77 (d, 1H), 9.22 (s, 1H), 9.53 (s, 1H). MS (ESI) m/z 462 [M + H]$^+$. HRMS [M + H]$^+$ = 462.1080 (theoretical 462.1066).

6′-(3-Ethylureido)-N′-hydroxy-4′-(4-(trifluoromethyl)thiazol-2-yl)-3,3′-bipyridine-5-carboximidamide (41). A mixture of 1-(5′-cyano-4-(4-(trifluoromethyl)thiazol-2-yl)-3,3′-bipyridin-6-yl)-3-ethylurea 40 (70 mg, 0.17 mmol) and hydroxylamine (0.015 mL, 0.25 mmol, 50% in water) in ethanol (3 mL) was heated to 80 °C for 1 h in a microwave reactor. Solvent was removed, and the residue was slurried in acetonitrile. Filtration of the solids and drying in vacuo gave the title compound as a white solid (52 mg, 69%). ^{1}H NMR (DMSO-d_6) δ 1.11 (t, 3H), 3.1–3.3 (m, 2H), 6.0 (s, 2H), 7.57 (brs, 1H), 8.03 (s, 1H), 8.26 (s, 1H), 8.35 (s, 1H), 8.46 (s, 1H), 8.56 (s, 1H), 8.93 (s, 1H), 9.48 (s, 1H), 9.1 (s, 1H). ^{13}C NMR (DMSO-d_6, 126 MHz) δ 166.0, 154.3, 153.9, 150.1, 149.2, 148.4, 146.0, 142.7, 139.3, 133.9, 131.6, 128.7, 126.4, 124.6, 120.4, 110.0, 33.9, 15.3. MS (ESI) m/z 452 [M + H]$^+$. HRMS [M + H]$^+$ = 452.1117 (theoretical 452.1111).

1-Ethyl-3-(5′-(5-oxo-4,5-dihydro-1,2,4-oxadiazol-3-yl)-4-(4-(trifluoromethyl)thiazol-2-yl)-3,3′-bipyridin-6-yl)urea (42). A mixture of compound 41 (70 mg, 0.16 mmol), DBU (0.023 mL, 0.16 mmol), and carbonyl diimidazole (25.1 mg, 0.16 mmol) in dioxane (3 mL) was stirred overnight at room temperature. The solvent was removed, and the residue was purified by reverse phase HPLC (Gilson, 25%ACN in water to 70% ACN with 0.1% TF) to give the title compound as a white solid (33 mg, 43%). ^{1}H NMR (DMSO-d_6) δ 1.09 (t, 3H), 3.1–3.3 (m, 2H), 7.51 (brs, 1H), 8.15 (s, 1H), 8.24 (s, 1H), 8.37 (s, 1H), 8.59 (s, 1H), 8.70 (s, 1H), 8.99 (d, 1H), 9.52 (s, 1H), 13.14 (brs, 1H). ^{13}C NMR (DMSO-d_6, 126 MHz) δ 166.1, 159.6, 155.5, 154.3, 154.2, 153.2, 149.4, 145.9, 142.9, 139.2, 134.9, 132.7, 126.3, 123.5, 119.5, 120.2, 110.4, 34.0, 15.3. MS (ESI) m/z 478 [M + H]$^+$. HRMS [M + H]$^+$ = 478.0924 (theoretical 478.0903).

Inhibition of ATPase Activity of Topoisomerase Enzymes. Assays for the ATPase activity of the various topoisomerase isozymes were performed as described previously[35,68] The ATPase activities of *E. coli* DNA gyrase and topoisomerase IV were measured from reconstituted tetramers of *E. coli* GyrA/GyrB and ParC/ParE, respectively. The ATPase activity of *S. aureus* DNA gyrase was measured from the reconstituted hybrid tetramer of the GyrB subunit from *S. aureus* with the GyrA subunit from *E. coli*. The *S. pneumoniae* topoisomerase IV ATPase assay was performed using the uncoupled GyrB subunit. Inhibition of ATPase activity was monitored by reduced production of inorganic phosphate, a product of the topoisomerase-catalyzed ATP hydrolysis reaction. Inorganic phosphate was quantified using the ammonium molybdate/malachite green-based detection system, measuring absorbance at 650 (A₆₅₀) nm, and assays were performed in microtiter plates containing of range concentrations of compounds dissolved in DMSO. For determination of the IC₅₀ values reported, raw A₆₅₀ nm was converted to percent inhibition calculated from the means of 32 wells each per assay plate of 0% inhibition (DMSO control) and 100% inhibition (2 μM novobiocin control)

wells. Curve fitting to determine IC₅₀ values was performed using the equation $\%I = 100/\{1 + (IC_{50}/[I])^n\}$.

Log D Determination. The partition coefficient (log D) was measured by shake flask method, using 10 mM phosphate buffer at pH 7.4 and *n*-octanol. The samples were allowed to reach equilibrium by shaking for 1 h at 1200 rpm, and sample analysis was done by LC/UV, with MS for mass confirmation.

pK_a Determination. pK_a values were determined at Sirius Analytical Instruments Ltd. (Forest Row Business Park, Station Road, Forest Row, East Sussex TH18 5DW, UK) by a Gold Standard pH metric assay on a Sirius T3 automated system in triplicate. The accuracy of the measurement was approximately 0.02 log units.

Plasma Protein Binding Determination. Human plasma protein binding was determined from a 10 μM compound solution in a Dianorm plasma well incubating at 37 °C for 16 h. Free fractions were calculated from ratios of drug concentration in buffer and plasma wells determined by LC-MS/MS.

Microsomal Clearance Determination. Metabolic stability was determined by incubating a 2 μM compound solution in 0.5 mg/mL human microsomes and adding 1 mM NADPH. Compound concentration at different time points was quantified by LC-MS/MS. Cl$_{int}$ was calculated from disappearance of the compound and correction factors.

Pharmacokinetic Studies. Pharmacokinetic properties of selected compounds were studied in male rats. Plasma pharmacokinetics were determined from 0 to 24 h following 15 min iv infusions at 10 mg/kg. Serial 200 μL samples of whole blood were taken at time intervals. Concentration of compound in plasma was determined by LC-MS/MS, and pharmacokinetic parameters were estimated using a noncompartmental model in WinNonLin (Pharsight). Mean results were determined from experiments with three mice.

Minimum Inhibitory Concentration (MIC). MIC values were determined by the broth microdilution method in accordance with the Clinical and Laboratory Standards Institute (CLSI) guidelines. In brief, bacterial suspensions were adjusted to a 0.5 McFarland standard to yield a final inoculum between 3×10^5 and 7×10^5 colony-forming units (CFU)/mL. For *S. aureus* strains (MSSA, wild-type from the AstraZeneca screening collection and MRQR, from the AstraZeneca screening collection),[57] bacterial inocula were made in sterile, cation adjusted Mueller–Hinton broth (Beckton Dickinson), and for *S. pneumoniae* (D39; NCTC 7466) in sterile, cation adjusted Mueller–Hinton broth containing 2.5% lysed horse blood (Hema Resource & Supply Inc.). For *E. coli* (W3110; ATCC 27325), *E. coli tolC⁻* (W3110 Δ*tolC*::Tn10 from the AstraZeneca screening collection),[57] *H. influenzae* (wild-type, Rd KW20; ATCC 51907), or *M. catarrhalis* (wild-type, ATCC43617) bacterial inocula were made in sterile, cation adjusted Mueller–Hinton broth (Beckton Dickinson) containing 0.5% yeast extract (Beckton Dickinson) plus 30 mL of 15 μg/mL Bovine Hematin stock (Sigma) and 3 mL of 15 μg/mL β-nicotinamide adenine dinucleotide (Sigma). An inoculum volume of 100 μL was added to wells (using a Tecan EVO robot) containing 2 μL of DMSO containing 2-fold serial dilutions of drug. All inoculated microdilution trays were incubated in ambient air at 35 °C for 18–24 h. Following incubation, the lowest concentration of the drug that prevented visible growth as read at OD600 nm was recorded as the MIC. Performance of the assay was monitored by the use of laboratory quality-control strains and commercially available control compounds with defined MIC spectra, in accordance with CLSI guidelines.

DNA Biosynthesis Inhibition. Incorporation of radiolabeled precursors (^{3}H-thymidine, ^{3}H-uridine, ^{14}C-leucine, ^{14}C-valine, ^{14}C-acetic acid and ^{14}C-*N*-acetyl glucosamine) of biological macromolecules was measured in *S. aureus* (MSSA) and *S. pneumoniae* (D39) following previously described methods.[32] The DNA gyrase inhibitor, ciprofloxacin, that inhibits DNA biosynthesis, was included as a reference.

Resistance Frequency and Isolation of Resistant Mutants. Resistance studies were performed following methods previously described.[28,45] Suspensions of bacterial cultures of methicillin-susceptible *S. aureus* (MSSA) were transferred onto Mueller–Hinton agar (BD, Franklin Lakes, NJ) plates containing compound at

Table 8. X-ray Data Processing and Refinement Statistics

	31	35
PDB code	4LP0	4LPB
Space group:	C222(1)	C222(1)
cell constants		
a, b, c (Å)	72.9, 94.3, 62.3	73.4, 94.7, 61.2
α, β, γ (deg)	90.0, 90.0, 90.0	90.0, 90.0, 90.0
resolution range (Å)	62.27−1.95 (2.06−1.95)	22.09−1.75
completeness overall (%)	99.8 (100.0)	99.9 (100)
reflections, unique	15830	21859
multiplicity	7.1 (7.3)	7.1 (7.2)
$R_{merge\ overall}$[a]	0.084 (0.386)	0.093 (0.577)
$R_{value\ overall}$ (%)[b]	17.6	21.8
$R_{value\ free}$ (%)[c]	20.8	23.6
non-hydrogen protein atoms	1511	1531
non-hydrogen ligand atoms	30	33
solvent molecules	107	120
rmsd from ideal values		
bond lengths (Å)	0.010	0.005
bond angles (deg)	1.39	1.08
Φ, Ψ angle distribution for residues[d]		
in most favored regions (%)	89.1	96.0
in additional allowed regions (%)	10.3	3.4
in generously regions (%)	0.0	0.0
in disallowed regions (%)	0.6	0.6

[a]$R_{merge} = \sum_{hkl} [(\sum_i |I_i - \langle I \rangle|)/\sum_i I_i]$. [b]$R_{value} = \sum_{hkl} ||F_{obs}| - |F_{calc}||/\sum_{hkl} |F_{obs}|$. [c]$R_{free}$ is the cross-validation R factor computed for the test set of 5% of unique reflections. [d]Ramachandran statistics as defined by PROCHECK.

multiples of the MIC (0.04 µg/mL) as well as plates without compound. The frequencies of resistance were calculated from the ratio of the number of colonies on the compound-containing plates divided by the number of colonies on compound-free plates following incubation for 7 days. Values from three separate plates were averaged to yield the reported frequency of spontaneous resistance. To ensure resistance stability, the recovered colonies were passaged twice on compound-free agar plates. Resistant strains that showed a significant shift in MIC as compared to the parental strain were further characterized by PCR amplification and sequencing of *gyrA, gyrB, parC,* and *parE* genes to identify mutations conferring resistance.

Generation of DNA Gyrase Mutations in *S. pneumoniae* and Cross-Resistance Determination. Point mutations in *gyrB* and *parE* genes in *S. pneumoniae* (D39; NCTC 7466) were generated as described previously.[28,45] Following similar methods, point mutations in *gyrA* and *parC* genes in *S. pneumoniae* were generated to create known fluoroquinolone-resistance mutations. MIC values of compounds against the parental strain and mutants of *S. pneumoniae* were determined following standard CLSI methods, as described above.

***S. pneumoniae* ParE Crystallization, X-ray Diffraction Data Collection and Refinement.** Crystals of the ATP binding domain of *S. pneumoniae* ParE (residues 1−226) were grown using vapor diffusion methodologies. A solution of 3 µL of 8 mg/mL protein in buffer containing 20 mM Tris pH 8.0, 100 mM NaCl was added to 3 µL of well solution (18−25% Peg4K, 0.2 M ammonium acetate, 0.1 M MIB, pH 7.0) and incubated at 16 °C. Crystals appeared within 3 days and grew to full size within 1 week. To create cocomplexes, crystals were transferred into a solution containing 25% Peg4000, 0.2 M ammonium acetate, 0.1 M MIB pH 7, and a 10% DMSO solution of **26** in buffer with a final compound concentration of 10 mM. Crystals were incubated for 6−24 h at 16 °C before a quick transfer into a cryosolution containing the soak solution and 2,3-butanediol (4.5:1 ratio) before freezing in liquid nitrogen. Data were collected at LRL-CAT. Indexing and data processing were performed using the autoPROC pipeline.[69] The molecular replacement solution was found using the program AMoRe[70] as implemented in the CCP4 suite of programs.[71] Iterative cycles of refinement and model building

were performed using Refmac[72] and COOT.[73] A summary of data collection and refinement statistics are listed in Table 8.

■ **AUTHOR INFORMATION**

Corresponding Author
*Phone: 781-839-4844. E-mail: greg.basarab@astrazeneca.com.

Present Addresses
§Epizyme, Inc., 400 Technology Square, Cambridge, Massachusetts 02139, United States.
‖EMD Serono Research and Development Institute, 45A Middlesex Turnpike, Billerica, Massachusetts 01821, United States.
‡Pfizer Worldwide Research and Development, 620 Memorial Drive, Cambridge, Massachusetts 02139, United States.
⊥Office of Biodefense, Research Resources & Translational Research, Division of Microbiology & Infectious Diseases, NIAID, NIH, 6610 Rockledge Drive, Bethesda, Maryland 20892, United States.

■ **ABBREVIATIONS USED**

CFU, colony-forming unit; GyrA, A-subunit of DNA gyrase; GyrB, B-subunit of DNA gyrase; LE, ligand efficiency; MSSA, methicillin sensitive *S. aureus*; MRQR, methicillin resistant,

quinolone resistant *S. aureus*; ParC, the C-subunit of topoisomerase IV; ParE, E-subunit of topoisomerase IV; *tolC*, gene encoding outer membrane transport channel

■ REFERENCES

(1) Bush, K.; Pucci, M. J. New antimicrobial agents on the horizon. *Biochem. Pharmacol.* **2011**, *82*, 1528−1539.

(2) Silver, L. L. Challenges of antibacterial discovery. *Clin. Microbiol. Rev.* **2011**, *24*, 71−109.

(3) Miller, J. R.; Waldrop, G. L. Discovery of novel antibacterials. *Expert Opin. Drug Discovery* **2010**, *5*, 145−154.

(4) Singh, S. B. Discovery and development of antibiotics with novel modes of action. *Spec. Publ.—R. Soc. Chem.* **2011**, *320*, 51−70.

(5) Hogberg, L. D.; Heddini, A.; Cars, O. The global need for effective antibiotics: challenges and recent advances. *Trends Pharmacol. Sci.* **2010**, *31*, 509−515.

(6) *FDA Approved Drugs*; CenterWatch: Boston, 2013; http://www.centerwatch.com/drug-information/fda-approvals.

(7) Blondeau, J. M. Tigecycline: an overview and update. *Therapy* **2009**, *6*, 851−870.

(8) Papp-Wallace, K. M.; Endimiani, A.; Taracila, M. A.; Bonomo, R. A. Carbapenems: past, present, and future. *Antimicrob. Agents Chemother.* **2011**, *55*, 4943−4960.

(9) El-Gamal, M. I.; Oh, C. H. Current status of carbapenem antibiotics. *Curr. Top. Med. Chem.* **2010**, *10*, 1882−1897.

(10) Malik, S.; Choudhary, A.; Kumar, S.; Avasthi, G. Quinolones: a therapeutic review. *J. Pharm. Res.* **2010**, *2*, 1519−1523.

(11) Black, M. T.; Coleman, K. New inhibitors of bacterial topoisomerase GyrA/ParC subunits. *Curr. Opin. Invest. Drugs* **2009**, *10*, 804−810.

(12) Alt, S.; Mitchenall, L. A.; Maxwell, A.; Heide, L. Inhibition of DNA gyrase and DNA topoisomerase IV of *Staphylococcus aureus* and *Escherichia coli* by aminocoumarin antibiotics. *J. Antimicrob. Chemother.* **2011**, *66*, 2061−2069.

(13) Fabrega, A.; Madurga, S.; Giralt, E.; Vila, J. Mechanism of action of and resistance to quinolones. *Microb. Biotechnol.* **2009**, *2*, 40−61.

(14) Bolon, M. K. The newer fluoroquinolones. *Med. Clin. North Am.* **2011**, *95*, 793−817 viii.

(15) Neuhauser, M. M.; Weinstein, R. A.; Rydman, R.; Danziger, L. H.; Karam, G.; Quinn, J. P. Antibiotic resistance among Gram-negative bacilli in US intensive care units: implications for fluoroquinolone use. *JAMA, J. Am. Med. Assoc.* **2003**, *289*, 885−888.

(16) Eagye, K. J.; Kuti, J. L.; Sutherland, C. A.; Christensen, H.; Nicolau, D. P. In vitro activity and pharmacodynamics of commonly used antibiotics against adult systemic isolates of *Escherichia coli* and *Pseudomonas aeruginosa* at Forty US Hospitals. *Clin. Ther.* **2009**, *31*, 2678−2688.

(17) Noel, G. J. A Review of Levofloxacin for the Treatment of Bacterial Infections. *Clin. Med. Insights: Ther.* **2009**, *1*, 433−458.

(18) Maxwell, A. The interaction between coumarin drugs and DNA gyrase. *Mol. Microbiol.* **1993**, *9*, 681−686.

(19) Byrskier, A.; Klich, M. Coumarin antibiotics: novobiocin, coumermycin, and clorobiocin. In *Antimicrobial Agents: Antibacterials and Antifungals*; Bryskier, A., Ed.; ASM Press: Washington, DC, 2005; pp 816−825.

(20) Skedelj, V.; Tomasic, T.; Masic, L. P.; Zega, A. ATP-binding site of bacterial enzymes as a target for antibacterial drug design. *J. Med. Chem.* **2011**, *54*, 915−929.

(21) Goetschi, E.; Angehrn, P.; Gmuender, H.; Hebeisen, P.; Link, H.; Masciadri, R.; Nielsen, J. Cyclothialidine and its congeners: a new class of DNA gyrase inhibitors. *Pharmacol. Ther.* **1993**, *60*, 367−380.

(22) Angehrn, P.; Goetschi, E.; Gmuender, H.; Hebeisen, P.; Hennig, M.; Kuhn, B.; Luebbers, T.; Reindl, P.; Ricklin, F.; Schmitt-Hoffmann, A. A New DNA Gyrase Inhibitor Subclass of the Cyclothialidine Family Based on a Bicyclic Dilactam-Lactone Scaffold. Synthesis and Antibacterial Properties. *J. Med. Chem.* **2011**, *54*, 2207−2224.

(23) Brvar, M.; Perdih, A.; Hodnik, V.; Renko, M.; Anderluh, G.; Jerala, R.; Solmajer, T. In silico discovery and biophysical evaluation of novel 5-(2-hydroxybenzylidene) rhodanine inhibitors of DNA gyrase B. *Bioorg. Med. Chem.* **2012**, *20*, 2572−2580.

(24) Lübbers, T.; Angehrn, P.; Gmünder, H.; Herzig, S.; Kulhanek, J. Design, synthesis, and structure−activity relationship studies of ATP analogues as DNA gyrase inhibitors. *Bioorg. Med. Chem. Lett.* **2000**, *10*, 821−826.

(25) Tari, L. W.; Trzoss, M.; Bensen, D. C.; Li, X.; Chen, Z.; Lam, T.; Zhang, J.; Creighton, C. J.; Cunningham, M. L.; Kwan, B.; Stidham, M.; Shaw, K. J.; Lightstone, F. C.; Wong, S. E.; Nguyen, T. B.; Nix, J.; Finn, J. Pyrrolopyrimidine inhibitors of DNA gyrase B (GyrB) and topoisomerase IV (ParE). Part I: Structure guided discovery and optimization of dual targeting agents with potent, broad-spectrum enzymatic activity. *Bioorg. Med. Chem. Lett.* **2013**, *23*, 1529−1536.

(26) Manchester, J. I.; Dussault, D. D.; Rose, J. A.; Boriack-Sjodin, P. A.; Uria-Nickelsen, M.; Ioannidis, G.; Bist, S.; Fleming, P.; Hull, K. G. Discovery of a novel azaindole class of antibacterial agents targeting the ATPase domains of DNA gyrase and topoisomerase IV. *Bioorg. Med. Chem. Lett.* **2012**, *22*, 5150−5156.

(27) Brvar, M.; Perdih, A.; Renko, M.; Anderluh, G.; Turk, D.; Solmajer, T. Structure-Based Discovery of Substituted 4,5′-Bithiazoles as Novel DNA Gyrase Inhibitors. *J. Med. Chem.* **2012**, *55*, 6413−6426.

(28) Uria-Nickelsen, M.; Neckermann, G.; Sriram, S.; Andrews, B.; Manchester, J. I.; Carcanague, D.; Stokes, S.; Hull, K. G. Novel topoisomerase inhibitors: microbiological characterisation and in vivo efficacy of pyrimidines. *Int. J. Antimicrob. Agents* **2013**, *41*, 363−371.

(29) Charifson, P. S.; Grillot, A. L.; Grossman, T. H.; Parsons, J. D.; Badia, M.; Bellon, S.; Deininger, D. D.; Drumm, J. E.; Gross, C. H.; LeTiran, A.; Liao, Y.; Mani, N.; Nicolau, D. P.; Perola, E.; Ronkin, S.; Shannon, D.; Swenson, L. L.; Tang, Q.; Tessier, P. R.; Tian, S. K.; Trudeau, M.; Wang, T.; Wei, Y.; Zhang, H.; Stamos, D. Novel dual-targeting benzimidazole urea inhibitors of DNA gyrase and topoisomerase IV possessing potent antibacterial activity: intelligent design and evolution through the judicious use of structure-guided design and structure−activity relationships. *J. Med. Chem.* **2008**, *51*, 5243−5263.

(30) Ronkin, S. M.; Badia, M.; Bellon, S.; Grillot, A.; Gross, C. H.; Grossman, T. H.; Mani, N.; Parsons, J. D.; Stamos, D.; Trudeau, M.; Wei, Y.; Charifson, P. S. Discovery of pyrazolthiazoles as novel and potent inhibitors of bacterial gyrase. *Bioorg. Med. Chem. Lett.* **2010**, *20*, 2828−2831.

(31) Starr, J. T.; Sciotti, R. J.; Hanna, D. L.; Huband, M. D.; Mullins, L. M.; Cai, H.; Gage, J. W.; Lockard, M.; Rauckhorst, M. R.; Owen, R. M.; Lall, M. S.; Tomilo, M.; Chen, H.; McCurdy, S. P.; Barbachyn, M. R. 5-(2-Pyrimidinyl)-imidazo[1,2-*a*]pyridines are antibacterial agents targeting the ATPase domains of DNA gyrase and topoisomerase IV. *Bioorg. Med. Chem. Lett.* **2009**, *19*, 5302−5306.

(32) East, S. P.; White, C. B.; Barker, O.; Barker, S.; Bennett, J.; Brown, D.; Boyd, E. A.; Brennan, C.; Chowdhury, C.; Collins, I.; Convers-Reignier, E.; Dymock, B. W.; Fletcher, R.; Haydon, D. J.; Gardiner, M.; Hatcher, S.; Ingram, P.; Lancett, P.; Mortenson, P.; Papadopoulos, K.; Smee, C.; Thomaides-Brears, H. B.; Tye, H.; Workman, J.; Czaplewski, L. G. DNA gyrase (GyrB)/topoisomerase IV (ParE) inhibitors: Synthesis and antibacterial activity. *Bioorg. Med. Chem. Lett.* **2009**, *19*, 894−899.

(33) Oblak, M.; Grdadolnik, S. G.; Kotnik, M.; Jerala, R.; Filipič, M.; Šolmajer, T. In silico fragment-based discovery of indolin-2-one analogues as potent DNA gyrase inhibitors. *Bioorg. Med. Chem. Lett.* **2005**, *15*, 5207−5210.

(34) Boehm, H.; Boehringer, M.; Bur, D.; Gmuender, H.; Huber, W.; Klaus, W.; Kostrewa, D.; Kuehne, H.; Luebbers, T.; Meunier-Keller, N.; Mueller, F. Novel Inhibitors of DNA Gyrase: 3D Structure Based Biased Needle Screening, Hit Validation by Biophysical Methods, and 3D Guided Optimization. A Promising Alternative to Random Screening. *J. Med. Chem.* **2000**, *43*, 2664−2674.

(35) Eakin, A. E.; Green, O.; Hales, N.; Walkup, G. K.; Bist, S.; Singh, A.; Mullen, G.; Bryant, J.; Embrey, K.; Gao, N.; Breeze, A.; Timms, D.; Andrews, B.; Uria-Nickelsen, M.; Demeritt, J.; Loch, J. T., 3rd; Hull, K.; Blodgett, A.; Illingworth, R. N.; Prince, B.; Boriack-Sjodin, P. A.; Hauck, S.; MacPherson, L. J.; Ni, H.; Sherer, B. Pyrrolamide DNA

gyrase inhibitors: fragment-based nuclear magnetic resonance screening to identify antibacterial agents. *Antimicrob. Agents Chemother.* **2012**, *56*, 1240−1246.

(36) Sherer, B. A.; Hull, K.; Green, O.; Basarab, G.; Hauck, S.; Hill, P.; Loch, J. T., III; Mullen, G.; Bist, S.; Bryant, J.; Boriack-Sjodin, A.; Read, J.; DeGrace, N.; Uria-Nickelsen, M.; Illingworth, R. N.; Eakin, A. E. Pyrrolamide DNA gyrase inhibitors: optimization of antibacterial activity and efficacy. *Bioorg. Med. Chem. Lett.* **2011**, *21*, 7416−7420.

(37) Wigley, D. B.; Davies, G. J.; Dodson, E. J.; Maxwell, A.; Dodson, G. Crystal structure of an N-terminal fragment of the DNA gyrase B protein. *Nature* **1991**, *351*, 624−629.

(38) Abad-Zapatero, C.; Perisic, O.; Wass, J.; Bento, A. P.; Overington, J.; Al-Lazikani, B.; Johnson, M. E. Ligand efficiency indices for an effective mapping of chemico-biological space: the concept of an atlas-like representation. *Drug Discovery Today* **2010**, *15*, 804−811.

(39) Sulavik, M. C.; Houseweart, C.; Cramer, C.; Jiwani, N.; Murgolo, N.; Greene, J.; DiDomenico, B.; Shaw, K. J.; Miller, G. H.; Hare, R.; Shimer, G. Antibiotic Susceptibility Profiles of *Escherichia coli* Strains Lacking Multidrug Efflux Pump Genes. *Antimicrob. Agents Chemother.* **2001**, *45*, 1126−1136.

(40) O'Shea, R.; Moser, H. E. Physicochemical Properties of Antibacterial Compounds: Implications for Drug Discovery. *J. Med. Chem.* **2008**, *51*, 2871−2878.

(41) Manchester, J. I.; Buurman, E. T.; Bisacchi, G. S.; McLaughlin, R. E. Molecular Determinants of AcrB-Mediated Bacterial Efflux Implications for Drug Discovery. *J. Med. Chem.* **2012**, *55*, 2532−2537.

(42) Grossman, T. H.; Bartels, D. J.; Mullin, S.; Gross, C. H.; Parsons, J. D.; Liao, Y.; Grillot, A. L.; Stamos, D.; Olson, E. R.; Charifson, P. S.; Mani, N. Dual targeting of GyrB and ParE by a novel aminobenzimidazole class of antibacterial compounds. *Antimicrob. Agents Chemother.* **2007**, *51*, 657−666.

(43) Tao, J.; Han, J.; Wu, H.; Hu, X.; Deng, J.; Fleming, J.; Maxwell, A.; Bi, L.; Mi, K. Mycobacterium fluoroquinolone resistance protein B, a novel small GTPase, is involved in the regulation of DNA gyrase and drug resistance. *Nucleic Acids Res.* **2013**, *41*, 2370−2381.

(44) Hilliard, J. J.; Goldschmidt, R. M.; Licata, L.; Baum, E. Z.; Bush, K. Multiple mechanisms of action for inhibitors of histidine protein kinases from bacterial two-component systems. *Antimicrob. Agents Chemother.* **1999**, *43*, 1693−1699.

(45) Mani, N.; Gross, C. H.; Parsons, J. D.; Hanzelka, B.; Müh, U.; Mullin, S.; Liao, Y.; Grillot, A.; Stamos, D.; Charifson, P. S.; Grossman, T. H. In Vitro Characterization of the Antibacterial Spectrum of Novel Bacterial Type II Topoisomerase Inhibitors of the Aminobenzimidazole Class. *Antimicrob. Agents Chemother.* **2006**, *50*, 1228−1237.

(46) Huang, W. M. Bacterial Diversity Based on Type II DNA Topoisomerase Genes. *Annu. Rev. Genet.* **1996**, *30*, 79−107.

(47) Brino, L.; Urzhumtsev, A.; Mousli, M.; Bronner, C.; Mitschler, A.; Oudet, P.; Moras, D. Dimerization of *Escherichia coli* DNA-gyrase B provides a structural mechanism for activating the ATPase catalytic center. *J. Biol. Chem.* **2000**, *275*, 9468−9475.

(48) Maxwell, A.; Lawson, D. M. The ATP-binding site of type II topoisomerases as a target for antibacterial drugs. *Curr. Top. Med. Chem.* **2003**, *3*, 283−303.

(49) Tsai, F. T.; Singh, O. M.; Skarzynski, T.; Wonacott, A. J.; Weston, S.; Tucker, A.; Pauptit, R. A.; Breeze, A. L.; Poyser, J. P.; O'Brien, R.; Ladbury, J. E.; Wigley, D. B. The high-resolution crystal structure of a 24-kDa gyrase B fragment from *E. coli* complexed with one of the most potent coumarin inhibitors, clorobiocin. *Proteins* **1997**, *28*, 41−52.

(50) Oblak, M.; Kotnik, M.; Solmajer, T. Discovery and Development of ATPase Inhibitors of DNA Gyrase as Antibacterial Agents. *Curr. Med. Chem.* **2007**, *14*, 2033−2047.

(51) Baba, T.; Takeuchi, F.; Kuroda, M.; Yuzawa, H.; Aoki, K.; Oguchi, A.; Nagai, Y.; Iwama, N.; Asano, K.; Naimi, T.; Kuroda, H.; Cui, L.; Yamamoto, K.; Hiramatsu, K. Genome and virulence determinants of high virulence community-acquired MRSA. *Lancet* **2002**, *359*, 1819−1827.

(52) Bax, B. D.; Chan, P. F.; Eggleston, D. S.; Fosberry, A.; Gentry, D. R.; Gorrec, F.; Giordano, I.; Hann, M. M.; Hennessy, A.; Hibbs, M.; Huang, J.; Jones, E.; Jones, J.; Brown, K. K.; Lewis, C. J.; May, E. W.; Saunders, M. R.; Singh, O.; Spitzfaden, C. E.; Shen, C.; Shillings, A.; Theobald, A. J.; Wohlkonig, A.; Pearson, N. D.; Gwynn, M. N. Type IIA topoisomerase inhibition by a new class of antibacterial agents. *Nature* **2010**, *466*, 935−942.

(53) Laponogov, I.; Sohi, M. K.; Veselkov, D. A.; Pan, X.; Sawhney, R.; Thompson, A. W.; McAuley, K. E.; Fisher, L. M.; Sanderson, M. R. Structural insight into the quinolone−DNA cleavage complex of type IIA topoisomerases. *Nature Struct. Mol. Biol.* **2009**, *16*, 667−669.

(54) Chopra, I.; Roberts, M. Tetracycline Antibiotics: Mode of Action, Applications, Molecular Biology, and Epidemiology of Bacterial Resistance. *Microbiol. Mol. Biol. Rev.* **2001**, *65*, 232−260.

(55) Munoz, R.; Bustamante, M.; De La Campa, A. Ser-127-to-Leu substitution in the DNA gyrase B subunit of *Streptococcus pneumoniae* is implicated in novobiocin resistance. *J. Bacteriol.* **1995**, *177* (14), 4166−4170.

(56) Bowker, K. E.; Garvey, M. I.; Noel, A. R.; Tomaselli, S. G.; MacGowan, A. P. Comparative antibacterial effects of moxifloxacin and levofloxacin on *Streptococcus pneumoniae* strains with defined mechanisms of resistance: impact of bacterial inoculum. *J. Antimicrob. Chemother.* **2013**, *68*, 1130−1138.

(57) Mills, S. D.; Eakin, A. E.; Buurman, E. T.; Newman, J. V.; Gao, N.; Huynh, H.; Johnson, K. D.; Lahiri, S.; Shapiro, A. B.; Walkup, G. K.; Yang, W.; Stokes, S. S. Novel bacterial NAD+-dependent DNA ligase inhibitors with broad-spectrum activity and antibacterial efficacy in vivo. *Antimicrob. Agents Chemother.* **2011**, *55*, 1088−1096.

(58) Vogelman, B.; Gudmundsson, S.; Leggett, J.; Turnidge, J.; Ebert, S.; Craig, W. A. Correlation of antimicrobial pharmacokinetic parameters with therapeutic efficacy in an animal model. *J. Infect. Dis.* **1988**, *158*, 831−847.

(59) Bist, S.; Eakin, A.; Sherer, B.; Zhao, S. Heterocyclic urea derivatives useful for treatment of bacterial infection. PCT Patent WO 2011024004, 2011.

(60) Choy, A. L.; Eakin, A.; Quiroga, O.; Sherer, B. Heterocyclic urea derivatives and methods of use thereof. PCT Patent WO 2010142978, 2010.

(61) Bifulco, N.; Choy, A. L.; Quiroga, O.; Sherer, B. Heterocyclic urea derivatives and methods of use thereof. PCT Patent WO 2010136817, 2010.

(62) Sherer, B.; Zhou, F. Heterocyclic urea derivatives and methods of use thereof. PCT Patent WO 2009147440, 2009.

(63) Hill, P.; Manchester, J. I.; Sherer, B.; Choy, A. L. Heterocyclic urea derivatives for the treatment of bacterial infections. WO 2009147433A1, 2009.

(64) . Bist, S.; Dangel, B.; Sherer, B. Heterocyclic urea derivatives and methods of use thereof-211. PCT Patent WO 2009106885, 2009.

(65) Basarab, G. S.; Bist, S.; Manchester, J. I.; Sherer, B. Chemical compounds. U.S. Patent US 20080132546, 2008.

(66) Norberto, F.; Santos, S.; Silva, D.; Herves, P.; Miguel, A. S.; Vilela, F. Reactivity of *N*-pyridylcarbamates in basic media. *J. Chem. Soc., Perkin Trans. 2* **2002**, 1162−1165.

(67) Oberwil, W. A.; Aesch, B. J. 3-Amino-2-mercaptobenzoic acid derivatives and processes for their preparation. U.S. Patent US 5770758, 1998.

(68) Reck, F.; Alm, R.; Brassil, P.; Newman, J.; DeJonge, B.; Eyermann, C. J.; Breault, G.; Breen, J.; Comita-Prevoir, J.; Cronin, M.; Davis, H.; Ehmann, D.; Galullo, V.; Geng, B.; Grebe, T.; Morningstar, M.; Walker, P.; Hayter, B.; Fisher, S. Novel N-Linked Aminopiperidine Inhibitors of Bacterial Topoisomerase Type II: Broad-Spectrum Antibacterial Agents with Reduced hERG Activity. *J. Med. Chem.* **2011**, *54*, 7834−7847.

(69) Vonrhein, C.; Flensburg, C.; Keller, P.; Sharff, A.; Smart, O.; Paciorek, W.; Womack, T.; Bricogne, G. Data processing and analysis with the autoPROC toolbox. *Acta Crystallogr., Sect. D: Biol. Crystallogr.* **2011**, *67*, 293−302.

(70) Navaza, J. AMoRe: an automated package for molecular replacement. *Acta Crystallogr., Sect. A: Found. Crystallogr.* **1994**, *50*, 157−163.

(71) Collaborative Computational Project, No. 4. The CCP4 suite: programs for protein crystallography. *Acta Crystallogr., Sect. D: Biol. Crystallogr.* **1994**, *50*, 760−763.

(72) Murshudov, G. N.; Vagin, A. A.; Dodson, E. J. Refinement of Macromolecular Structures by the Maximum-Likelihood Method. *Acta Crystallogr., Sect. D: Biol. Crystallogr.* **1997**, *53*, 240−255.

(73) Emsley, P.; Lohkamp, B.; Scott, W. G.; Cowtan, K. Features and development of Coot. *Acta Crystallogr., Sect. D: Biol. Crystallogr.* **2010**, *66*, 486−501.